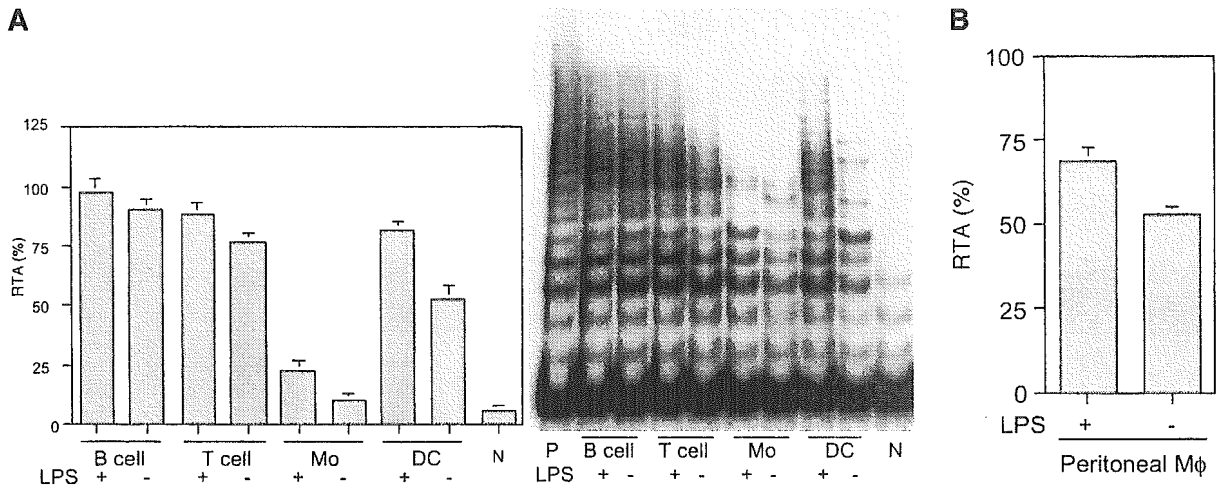

Fig. 2. Effect of LPS on telomerase activities of splenic cells and peritoneal macrophages. (A) LPS or PBS was injected i.p. into mice. After 48 h, splenic cells were sorted by antibody microbeads and separated to DCs by anti-CD11c, monocytes (Mo) by anti-CD11b, T cells by anti-CD90, and B cells by anti-CD19. ELISA and TRAP measured telomerase activity of each population. P, positive control; N, negative control. (B) After LPS or PBS injection, ELISA measured telomerase activity of peritoneal macrophages (M).

cells between young and old mice. Although telomerase activity of lymphoid cells (B and T cells) was mostly comparable, that of DCs in old mice was significantly higher than young mice ($P<0.01$; **Fig. 3A**). Furthermore, splenic DCs from old mice rather decreased the telomerase activity after in vitro stimulation with LPS, although those from young mice showed a slight increase of ~10%. By FACS analysis, freshly isolated, splenic DCs from both generations showed similar cell-surface phenotype determined by CD11c, MHC class II, and CD86 expression (Fig. 3B). However after stimulation, expression of activation markers such as MHC class II and CD86 was apparently lower in old mice, indicating poor responses to LPS (Fig. 3B). We also tried in vivo stimulation by injection of LPS, but old mice were not resistant and died (data not shown).

Next, we compared the telomerase activities of BM DCs (**Fig. 4**). We generated imDCs in the same set of in vitro cultures of BM cells from young mice (6 week), adult mice (1 year), and old mice (2 years). Contrary to the results of splenic DCs, BM DCs from old mice had consistently lower telomerase activity than those from young and adult mice, both of which

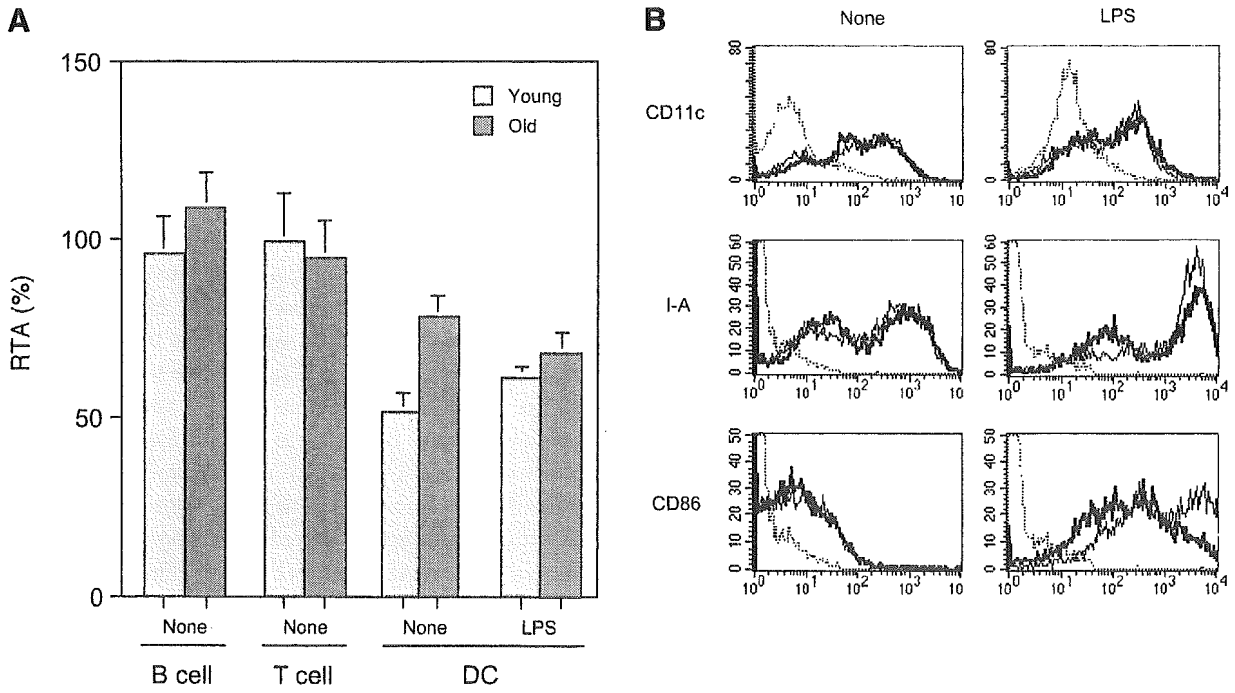

Fig. 3. Comparison of telomerase activity and surface phenotye of splenic DCs between young and old mice. (A) Telomerase activities of freshly isolated splenic B cells, T cells, DCs, and LPS-stimulated DCs were compared between young and old mice. (B) Expression of CD11c and activation markers of DCs [MHC class II (I-A) and CD86] was measured by fluorescein-activated cell sorter (FACS) in freshly isolated splenic DCs and LPS-stimulated DCs from young (thin line) and old (bold line) mice. Background staining with irrelevant Ab was expressed by the dotted line.

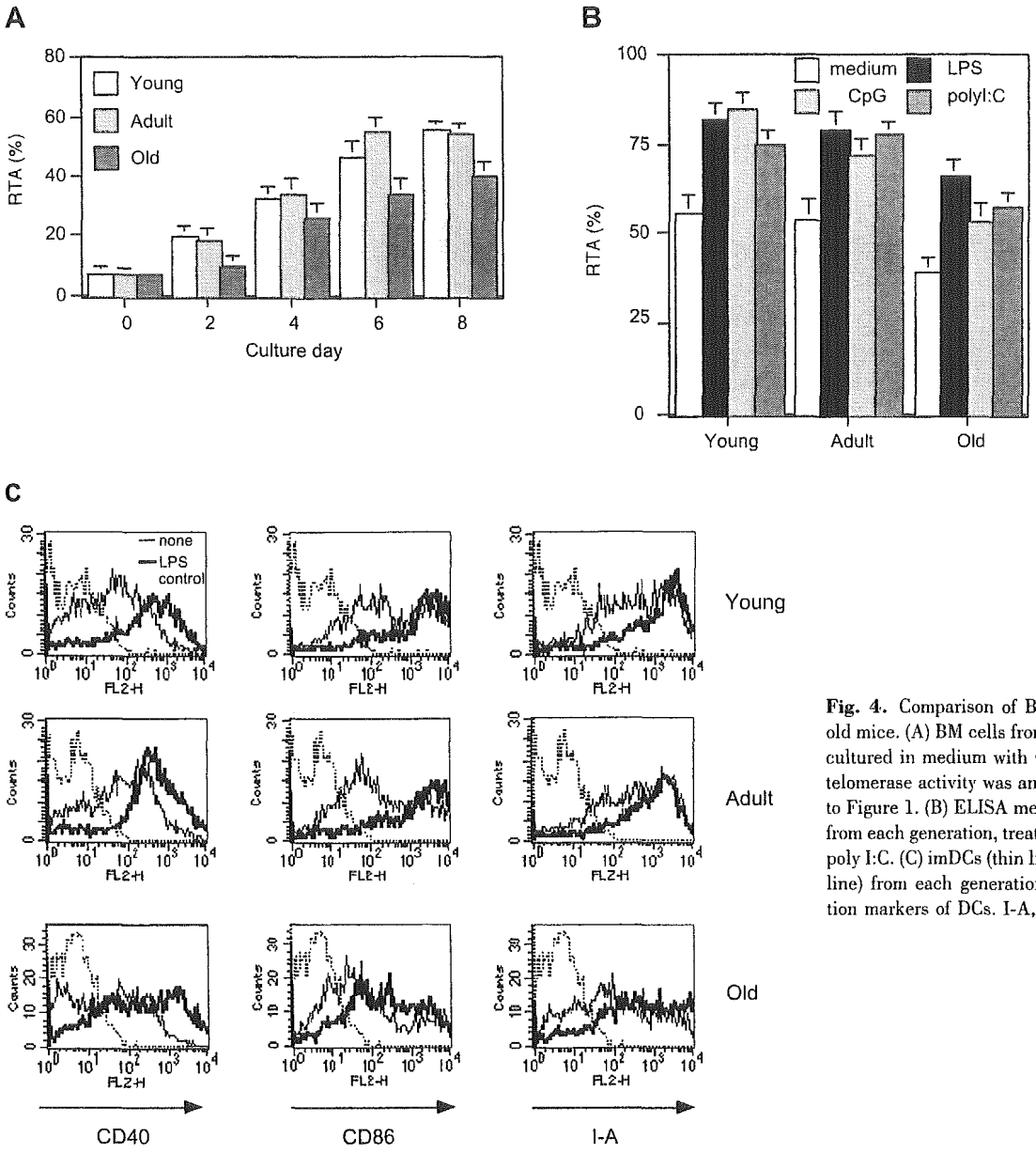

Fig. 4. Comparison of BM DCs among young, adult, and old mice. (A) BM cells from old, adult, and young mice were cultured in medium with GM-CSF and IL-4. Every 2 days, telomerase activity was analyzed as described in the legend to Figure 1. (B) ELISA measured telomerase activity of DCs from each generation, treated or untreated with LPS, CpG, or poly I:C. (C) imDCs (thin line) and LPS-induced mDCs (bold line) from each generation measured expression of activation markers of DCs. I-A, MHC class II.

had similar activity (Fig. 4A). At day 6, imDCs from each generation were stimulated with LPS, CpG-ODN, or poly I:C to induce maturation. In this experiment, up-regulation of telomerase activity after stimulation was observed in all generations, but still, the lowest activity in old mice was consistent (Fig. 4B). By FACS analysis, expression of activation markers such as CD40, CD86, and MHC class II was lower in old mice, and this tendency became more significant after stimulation (Fig. 4C). Thus, lower telomerase activity of BM DCs in old mice seemed associated with insufficient activation.

DISCUSSION

Telomerase in DCs

Telomere has an essential role in stabilizing chromosome ends and in preventing end-to-end fusions, and its expression has been found to correlate with cell proliferation in many different types of cells. Thus, telomerase activation is important in determining the proliferative capacity of cells and counteracts telomere loss. Telomerase activity has been shown to increase upon activation of T and B cells; however, a limited number of studies showed the telomere length and telomerase activity in myeloid-lineage cells. It was reported that telomerase activity was up-regulated in mature myeloid progenitors by plating in cultures supplemented with IL-3, Flt3-ligand, and stem-cell factor, and telomerase activity was also induced during development of human mast cells from peripheral blood $CD34^+$ cells [26, 27]. GM-CSF was shown to suppress the telomerase activity and telomerase reverse transcriptase (TERT) expression by synergistic effect with retinoic acid in myeloid leukemia cells [28]. Thus, it raises the question as to whether DCs change telomerase activity during differentiation as a professional APC.

Here, we clearly demonstrated that telomerase activity is largely increased during the differentiation and maturation

process of DCs. In in vitro induction of DCs with GM-CSF and IL-4, telomerase activity was low at the beginning in the whole extract from BM cells but gradually increased during differentiation into $CD11c^+$ imDCs (Fig. 1). When LPS, CpG-ODN, and dsRNA induced DC maturation, telomerase activity of imDCs, having a moderate level, rose to the peak after maturation. All microbial products we used for DC maturation transduced activation signals through the TLR pathway. TLRs used the same signaling molecules including MyD88, IL-1 receptor-associated protein kinase, and tumor necrosis factor (TNF) receptor-associated factor 6, leading to the activation of nuclear factor (NF)-κB [10]. The fact that the mouse TERT promoter is regulated by the widely expressed and highly inducible NF-κB transcription factor further supports our findings of telomerase activation in DC maturation [29]. However, the physiological role of the inducible telomerase activity is still unclear. In addition to the well-characterized action of telomerase in adding telomeric repeats, it should be noted that recent studies suggest that telomerase may have additional functions, for example, in protecting cellular, proliferative capacity and in preventing apoptosis without telomere elongation [30]. Actually in our experiments, during differentiation to mDCs from imDCs by microbial components, telomerase activity was increased without cellular proliferation (data not shown). Engagement of TLRs, CD40L, or TNF-related activation-induced cytokine receptor enhances longevity of DCs through NF-κB activation [31, 32], which also positively controls telomerase expression. Considering recent findings that LPS and CpG not only mature DCs but also inhibit DC apoptosis [33, 34], telomerase activation may contribute to this antiapoptotic effect. In addition, DCs were reported to be targets of cytotoxic T cell and NK cell-mediated killing, and activation of DCs by LPS or CD40 renders DCs resistant to the cytotoxicity [35, 36]. Taken together, the inducible telomerase activity could be a key component to potentiate DC function, proliferation, and survival.

DCs in aged mice

Despite numerous, recent advances in the molecular and cellular biology of DCs, very few groups have addressed the topic of DCs and aging [37]. In animal models of old mice, DCs of lymph nodes showed degenerative characteristics with decreased adhesion molecule expression, less dendrite formation, and reduced antigen-trapping capacity, which together, imply disruption of functional activity [38]. In contrast, DCs generated from peripheral blood of elderly people were not impaired in their capacity to induce cell responses [39]. During aging, however, it is obvious that there is a marked decline in the reactivity of the immune system, which has been attributed to impairment of lymphocyte function in corporation with innate-immune responses [40, 41]. Here, we observed that splenic DCs in old mice possessed much higher telomerase activity than young mice but even decreased the activity after LPS stimulation (Fig. 3A). On the contrary, BM DCs from old mice had considerably lower telomerase activity than those from younger ones and remained weaker after stimulation with microbial components, together with lower activation marker expression (Fig. 4). Thus, splenic DCs and BM DCs have the different nature in old mice. The mechanisms and physiological meanings underlying this contradicting data between splenic and BM DCs are still to be investigated. As lower telomerase activity of BM DCs in old mice seemed associated with an insufficiently activated status (Fig. 4C), it may reflect inferior differentiation and regeneration potential of BM cells. Conversely, peripheral splenic DCs in old mice may be compensating for something such as telomere shortening or functional defects of DCs and implying a terminal stage in cell fate. However, poor responses of expression of activation markers to LPS stimulation were consistent in splenic and BM DCs (Figs. 3B and 4C). In any case, DCs in old mice have a different feature from younger mice, and these may contribute to the pathogenesis and poor resistance to infection or endotoxin shock accompanied with aging

This is the first report to investigate the telomerase activity in DCs and make a comparison between young and old mice. Our observations would provide a new insight regarding immunobiology and immunosenescense. Analysis of DCs in telomerase knockout mice ($mTERT^{-/-}$) [42] will clarify the physiological roles of telomerase in immunity.

ACKNOWLEDGMENTS

The study was supported by the Fund for Comprehensive Research on Aging and Health, the Research Grant for Longevity Sciences (13C-1) from the Ministry of Health and Welfare, the Program for Promotion of Fundamental Studies in Health Sciences of the Organization for Pharmaceutical Safety and Research, a grant from Japan Health Science Foundation, and grant-in-aids for Scientific Research from the Ministry of Education and Uehara Memorial Foundation. We thank Dr. Kerry S. Campbell and Akiko Maki (Fox Chase Cancer Center, Philadelphia, PA) for critically reading the manuscript and helpful discussion.

REFERENCES

1. Steinman, R. M. (1991) The dendritic cell system and its role in immunogenicity. *Annu. Rev. Immunol.* **9**, 271–296.
2. Banchereau, J., Briere, F., Caux, C., Davoust, J., Lebecque, S., Liu, Y. J., Pulendran, B., Palucka, K. (2000) Immunobiology of dendritic cells. *Annu. Rev. Immunol.* **18**, 767–811.
3. Cella, M., Engering, A., Pinet, V., Pieters, J., Lanzavecchia, A. (1997) Inflammatory stimuli induce accumulation of MHC class II complexes on dendritic cells. *Nature* **388**, 782–787.
4. Pierre, P., Turley, S. J., Gatti, E., Hull, M., Meltzer, J., Mirza, A., Inaba, K., Steinman, R. M., Mellman, I. (1997) Developmental regulation of MHC class II transport in mouse dendritic cells. *Nature* **388**, 787–792.
5. Sallusto, F. (2001) Origin and migratory properties of dendritic cells in the skin. *Curr. Opin. Allergy Clin. Immunol.* **1**, 441–448.
6. Lanzavecchia, A., Sallusto, F. (2001) Regulation of T cell immunity by dendritic cells. *Cell* **106**, 263–266.
7. Rescigno, M., Granucci, F., Citterio, S., Foti, M., Ricciardi-Castagnoli, P. (1999) Coordinated events during bacteria-induced DC maturation. *Immunol. Today* **20**, 200–203.
8. Cella, M., Salio, M., Sakakibara, Y., Langen, H., Julkunen, I., Lanzavecchia, A. (1999) Maturation, activation, and protection of dendritic cells induced by double-stranded RNA. *J. Exp. Med.* **189**, 821–829.
9. Kadowaki, N., Antonenko, S., Liu, Y. J. (2001) Distinct CpG DNA and polyinosinic-polycytidylic acid double-stranded RNA, respectively, stimulate CD11c-type 2 dendritic cell precursors and CD11c+ dendritic cells to produce type I IFN. *J. Immunol.* **166**, 2291–2295.

10. Akira, S., Takeda, K., Kaisho, T. (2001) Toll-like receptors: critical proteins linking innate and acquired immunity. *Nat. Immunol.* **2,** 675–680.
11. Greider, C. W. (1996) Telomere length regulation. *Annu. Rev. Biochem.* **65,** 337–365.
12. Blackburn, E. H. (2001) Switching and signaling at the telomere. *Cell* **106,** 661–673.
13. Hastie, N. D., Dempster, M., Dunlop, M. G., Thompson, A. M., Green, D. K., Allshire, R. C. (1990) Telomere reduction in human colorectal carcinoma and with ageing. *Nature* **346,** 866–868.
14. Blackburn, E. H. (2000) Telomere states and cell fates. *Nature* **408,** 53–56.
15. Hackett, J. A., Feldser, D. M., Greider, C. W. (2001) Telomere dysfunction increases mutation rate and genomic instability. *Cell* **106,** 275–286.
16. Bodnar, A. G., Ouellette, M., Frolkis, M., Holt, S. E., Chiu, C. P., Morin, G. B., Harley, C. B., Shay, J. W., Lichtsteiner, S., Wright, W. E. (1998) Extension of life-span by introduction of telomerase into normal human cells. *Science* **279,** 349–352.
17. Vaziri, H., Benchimol, S. (1998) Reconstitution of telomerase activity in normal human cells leads to elongation of telomeres and extended replicative life span. *Curr. Biol.* **8,** 279–282.
18. Buchkovich, K. J., Greider, C. W. (1996) Telomerase regulation during entry into the cell cycle in normal human T cells. *Mol. Biol. Cell* **7,** 1443–1454.
19. Bodnar, A. G., Kim, N. W., Effros, R. B., Chiu, C. P. (1996) Mechanism of telomerase induction during T cell activation. *Exp. Cell Res.* **228,** 58–64.
20. Ogoshi, M., Takashima, A., Taylor, R. S. (1997) Mechanisms regulating telomerase activity in murine T cells. *J. Immunol.* **158,** 622–628.
21. Hathcock, K. S., Weng, N. P., Merica, R., Jenkins, M. K., Hodes, R. (1998) Cutting edge: antigen-dependent regulation of telomerase activity in murine T cells. *J. Immunol.* **160,** 5702–5706.
22. Herrera, E., Martinez, A. C., Blasco, M. A. (2000) Impaired germinal center reaction in mice with short telomeres. *EMBO J.* **19,** 472–481.
23. Inaba, K., Inaba, M., Romani, N., Aya, H., Deguchi, M., Ikehara, S., Muramatsu, S., Steinman, R. M. (1992) Generation of large numbers of dendritic cells from mouse bone marrow cultures supplemented with granulocyte/macrophage colony-stimulating factor. *J. Exp. Med.* **176,** 1693–1702.
24. Kadowaki, N., Ho, S., Antonenko, S., Malefyt, R. W., Kastelein, R. A., Bazan, F., Liu, Y. J. (2001) Subsets of human dendritic cell precursors express different Toll-like receptors and respond to different microbial antigens. *J. Exp. Med.* **194,** 863–869.
25. De Smedt, T., Pajak, B., Muraille, E., Lespagnard, L., Heinen, E., De Baetselier, P., Urbain, J., Leo, O., Moser, M. (1996) Regulation of dendritic cell numbers and maturation by lipopolysaccharide in vivo. *J. Exp. Med.* **184,** 1413–1424.
26. Yui, J., Chiu, C. P., Lansdorp, P. M. (1998) Telomerase activity in candidate stem cells from fetal liver and adult bone marrow. *Blood* **91,** 3255–3262.
27. Chaves-Dias, C., Hundley, T. R., Gilfillan, A. M., Kirshenbaum, A. S., Cunha-Melo, J. R., Metcalfe, D. D., Beaven, M. A. (2001) Induction of telomerase activity during development of human mast cells from peripheral blood CD34+ cells: comparisons with tumor mast-cell lines. *J. Immunol.* **166,** 6647–6656.
28. Mano, Y., Shimizu, T., Tanuma, S., Takeda, K. (2000) Synergistic down-regulation of telomerase activity and hTERT mRNA expression by combination of retinoic acid and GM-CSF in human myeloblastic leukemia ML-1 cells. *Anticancer Res.* **20,** 1649–1652.
29. Yin, L., Hubbard, A. K., Giardina, C. (2000) NF-kappa B regulates transcription of the mouse telomerase catalytic subunit. *J. Biol. Chem.* **275,** 36671–36675.
30. Fu, W., Begley, J. G., Killen, M. W., Mattson, M. P. (1999) Anti-apoptotic role of telomerase in pheochromocytoma cells. *J. Biol. Chem.* **274,** 7264–7271.
31. Ghosh, S., May, M. J., Kopp, E. B. (1998) NF-kappa B and Rel proteins: evolutionarily conserved mediators of immune responses. *Annu. Rev. Immunol.* **16,** 225–260.
32. Ouaaz, F., Arron, J., Zheng, Y., Choi, Y., Beg, A. A. (2002) Dendritic cell development and survival require distinct NF-kappaB subunits. *Immunity* **16,** 257–270.
33. Ardeshna, K. M., Pizzey, A. R., Devereux, S., Khwaja, A. (2000) The PI3 kinase, p38 SAP kinase, and NF-kappaB signal transduction pathways are involved in the survival and maturation of lipopolysaccharide-stimulated human monocyte-derived dendritic cells. *Blood* **96,** 1039–1046.
34. Park, Y., Lee, S. W., Sung, Y. C. (2002) Cutting edge: CpG DNA inhibits dendritic cell apoptosis by up-regulating cellular inhibitor of apoptosis proteins through the phosphatidylinositide-3′-OH kinase pathway. *J. Immunol.* **168,** 5–8.
35. Medema, J. P., Schuurhuis, D. H., Rea, D., van Tongeren, J., de Jong, J., Bres, S. A., Laban, S., Toes, R. E., Toebes, M., Schumacher, T. N., Bladergroen, B. A., Ossendorp, F., Kummer, J. A., Melief, C. J., Offringa, R. (2001) Expression of the serpin serine protease inhibitor 6 protects dendritic cells from cytotoxic T lymphocyte-induced apoptosis: differential modulation by T helper type 1 and type 2 cells. *J. Exp. Med.* **194,** 657–667.
36. Ronchese, F., Hermans, I. F. (2001) Killing of dendritic cells: a life cut short or a purposeful death? *J. Exp. Med.* **194,** F23–F26.
37. Saurwein-Teissl, M., Romani, N., Grubeck-Loebenstein, B. (2000) Dendritic cells in old age–neglected by gerontology? *Mech. Ageing Dev.* **121,** 123–130.
38. Grewe, M. (2001) Chronological ageing and photoageing of dendritic cells. *Clin. Exp. Dermatol.* **26,** 608–612.
39. Lung, T. L., Saurwein-Teissl, M., Parson, W., Schonitzer, D., Grubeck-Loebenstein, B. (2000) Unimpaired dendritic cells can be derived from monocytes in old age and can mobilize residual function in senescent T cells. *Vaccine* **18,** 1606–1612.
40. Globerson, A., Effros, R. B. (2000) Ageing of lymphocytes and lymphocytes in the aged. *Immunol. Today* **21,** 515–521.
41. Weng, N. (2001) Interplay between telomere length and telomerase in human leukocyte differentiation and aging. *J. Leukoc. Biol.* **70,** 861–867.
42. Xunmei, Y., Nikaido, R., Haruyama, T., Watanabe, Y., Iwata, H., Iida, M., Sugimura, H., Yamada, N., Ishikawa, F. (1999) Presence of telomeric G-strand tails in the telomerase catalytic subunit TERT knockout mice. *Genes Cells* **4,** 563–572.

Journal of Cellular Biochemistry 90:1242–1249 (2003)

GADD34 Induces p53 Phosphorylation and p21/WAF1 Transcription

Ayako Yagi,[1,2] Yoshinori Hasegawa,[2] Hengyi Xiao,[1] Masataka Haneda,[1] Eiji Kojima,[1,2] Akihiko Nishikimi,[1] Tadao Hasegawa,[1] Kaoru Shimokata,[2] and Ken-Ichi Isobe[1]*

[1]Department of Basic Gerontology, National Institute for Longevity Sciences, Morioka-cho, Obu, Aichi 474-8522, Japan
[2]Department of Internal Medicine, Nagoya University Graduate School of Medicine, Tsurumai-cho, Showa-ku, Nagoya, Aichi 466-8520, Japan

Abstract Recently, others and we have shown that one of the functions of GADD34 is a recovery from a shutoff of protein synthesis induced by endoplasmic reticulum stress. GADD34 has been shown to induce growth arrest and apoptosis. Main protein of apoptosis is p53, especially phosphorylation of p53. And one of the main proteins of growth arrest is p21/WAF1. Here we analyzed the effects of GADD34 on p53 phosphorylation and p21/WAF1 transcription. Transfected Myc-tagged p53 was dose-dependently phosphorylated at Ser15 by increasing the amount of GADD34. Transfection of GADD34 also induced the endogenous phosphorylation of p53 and enhanced p21 protein expression. Transfection of GADD34 induced p21/WAF1 promoter activity. This activity was dependent on p53, because GADD34 transfection to p53-deficient cells produced only a slight increase of p21/WAF1 promoter activity. The p21/WAF1 promoter activity was greatly enhanced by the transfection of p53. Both GADD34 and p53 transfection induced much higher p21/WAF1 promoter activity. The promoter activity of p21/WAF1 was very low in GADD34 deficient MEF. The transfection of GADD34 increased the p21/WAF1 promoter activity in GADD34 deficient MEF. J. Cell. Biochem. 90: 1242–1249, 2003.

Key words: GADD34; p53; p21/WAF1

GADD34 is a member of the protein family whose expression is up regulated by growth arrest and DNA damage [Zhan et al., 1994]. GADD34, like GADD45 and GADD153, was originally discovered as an UV-inducible transcript in Chinese hamster ovary cells [Fornace et al., 1989]. A later study demonstrated a correlation between the onset of apoptosis and GADD34 expression in selected cell lines following ionizing irradiation or treatment with the alkylating agent methyl methanesulfate [Hollander et al., 1997]. GADD34 is also induced by amino acid deprivation and several endoplasmic reticulum (ER) stresses [Mengesdorf et al., 2001; Novoa et al., 2001]. GADD34 harbors a highly conserved domain in its carboxyl-terminus, which is homologous to $\gamma_1$34.5 of HSV1. $\gamma_1$34.5 is a virulence factor that blocks the premature shutoff of protein synthesis in HSV1-infected neuroblastoma cells [Chin et al., 1997]. The carboxyl-terminal domain of the $\gamma_1$34.5 protein binds to protein phosphatase 1 (PP1). This complex specifically dephosphorylates eukaryotic translation initiation factor 2 α (eIF2α), which is evolved to preclude a shutoff of protein synthesis [He et al., 1998]. These findings suggest two possible function of cellular GADD34. One is related to apoptosis or cell cycle arrest. Another is related to shutoff of protein synthesis. Recently, we [Kojima et al., 2003] and other group [Novoa et al., 2003] have shown the latter function of GADD34 in vivo by using GADD34 knockout mice. We have shown that in GADD34$^{-/-}$ mouse embryonic fibroblasts (MEFs), recovery from a shutoff of protein synthesis was delayed, when MEF were exposed to endoplasmic reticulum (ER) stress [Kojima et al., 2003]. Several studies have demonstrated that the onset of apoptosis

*Correspondence to: Ken-Ichi Isobe, MD, PhD, Department of Basic Gerontology, National Institute for Longevity Sciences, 36-3, Gengo, Morioka-cho, Obu, Aichi 474-8522, Japan. E-mail: kenisobe@nils.go.jp

Received 3 September 2003; Accepted 4 September 2003
DOI 10.1002/jcb.10711
Published online 6 November 2003 in Wiley InterScience (www.interscience.wiley.com).

is correlated with GADD34 expression in selected cell lines after ionizing irradiation or alkylating agent of methyl methanesulfate treatment [Adler et al., 1999; Grishin et al., 2001]. HRX leukemic fusion oncogenes, the human homologue of the *Drosophila trithorax* (*trx*) gene, binds GADD34 to negatively regulate the apoptotic response [Adler et al., 1999] The expression of GADD34 in the colorectal cancer cell line SW480 has been reported to enhance IR-induced apoptosis [Adler et al., 1999]. Several proteins have been shown to be associated with GADD34. An association with proliferating cell nuclear antigen suggests that GADD34 might inhibit proliferation [Brown et al., 1997]. We have shown that GADD34 interacts with Zfp148 (also known as BFCOL1), which might affect p21/WAF1 transcription [Hasegawa et al., 1999]. Bai and Merchant [2001] have demonstrated that Zfp148 enhances p53 transcriptional activity and prevents p53 degradation by binding to p53 via its zinc-finger domain. Overexpression of Zfp148 leads to an accumulation of p53 in the nucleus, activation of p21/WAF1 and cell cycle arrest. Recently, we have shown that Zfp148 plays an essential role in the differentiation of fetal germ cells by stimulating the phosphorylation of p53 at Ser15 [Takeuchi et al., 1997]. These results indicate that GADD34 induces p21/WAF1 transcription via p53. Here, we show that transfection of GADD34 induces the phosphorylation of p53 at Ser15, and induces p21/WAF1 transcription via p53 binding site.

MATERIALS AND METHODS

Cell Culture

BALB3T3 10(1) cells were p53-deficient mouse fibroblast cell line, which were kindly donated from Dr. Arnold J. Levine [Harvey and Levine, 1991]. NIH3T3, 293 and 10(1) cells were maintained in Dulbecco's modified Eagle's medium (Sigma, St. Louis, MO) supplemented

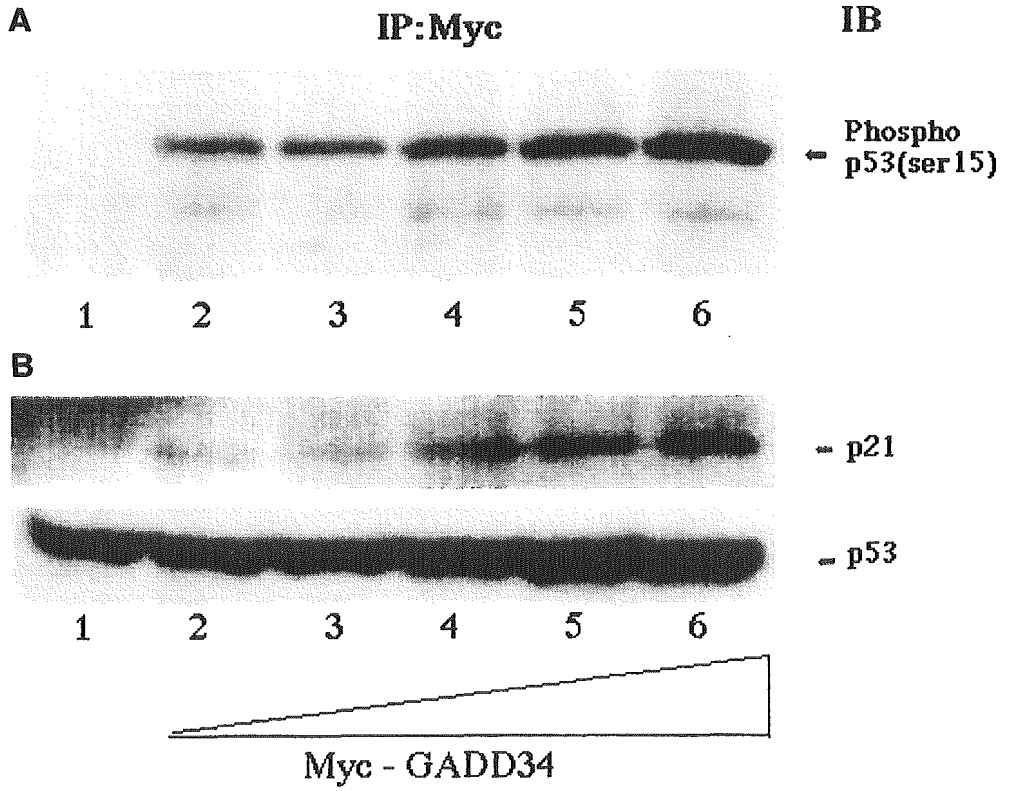

Fig. 1. Induction of p53 phosphorylation by GADD34 transfection. **A**: 293 cells were transfected with 1.0 μg of Myc-tagged vector (**lane 1**). Two hundred ninety-three cells were transfected with 0.5 μg of Myc-tagged p53 expression vector (**lanes 2–6**), together with increasing amount of Myc-tagged GADD34 expression vector (lanes 2–6; 0, 0.05, 0.1, 0.25, 0.5 μg) in six tissue culture wells. Immunoprecipitations were carried out with anti-Myc antibodies followed by immunoblot analysis with phospho-p53 (Ser 15) antibodies. **B**: Two hundred ninety-three cells were transfected with increasing amount of GADD34 expression vector (lanes 1–6; 0, 0.05, 0.1, 0.25, 0.5, 1.0 μg). Lysates were analyzed for the expression of the proteins by immunoblotting with p21/WAF1and p53 antibodies.

with 10% fetal bovine serum, 100 U/ml penicillin, and 100 μg/ml streptomycin. MEFs were prepared from 14.5-day embryos of GADD34 knockout and wild-type control mice [Kojima et al., 2003]. The cultures were maintained in Dulbecco's modified essential medium with 10% FCS. Cells were plated $1-2 \times 10^6$/10 cm plate for subculture and experimentation.

Plasmid Constructs

The mouse p21/WAF1 promoter luciferase reporter plasmids and the mutant of p53-binding site (mutants 1; p21 (−1)) were constructed as described previously [Xiao et al., 1997, 1999]. Full-length cDNA of GADD34 was constructed by mRNA of NIH3T3 cells. We used RT-PCR using sense primer as GGAATTCCAGACACATGCCCCCGAGC and antisense primer as ACGCGTCGACGCCCCGCCTCCCAAG. They were cut with *Xba*I/*Hin*III and inserted into partial GADD34 expression vector [Hasegawa et al., 1999] based on pcDNA3.1/Myc-His A vector (Invitrogen, Bethesda, MA). Myc-His tagged p53 expression vector was constructed from the p53 cDNA donated from Dr. Vogelstein, We used GCTCTAGATGGAGGAGCCGCAG (sense) and CCCAAGCTTGTCTGAGTCAGGCCCTTCTGT (antisense) for PCR primers and p53 cDNA as target. The PCR product was cut with *Xba*I/*Hin*D and inserted into Myc-His tagged (Invitrogen). pTA-luc vectors were purchased from Clontech (Palo Alto, CA). The pTA-luc contains the firefly luciferase (*Luc*) gene fused to a TATA-like (TAL) promoter region from the Herpes simplex virus thymidine kinase (HSV-TK) promoter. The pp53TA-Luc (Tal-p53) contains the firefly luciferase gene and has the p53-binding sequence fused to pTA-luc vector.

Transfection Assays

Transient transfection to 293, NIH3T3 and 10(1) cells was carried out using SuperFect reagent (Qiagen, Hilden, Germany) as previously described [Maehara et al., 2001]. In general, the day before transfection, 2×10^5 cells were plated in 24-well tissue culture plates. A total of 0.5–0.6 μg of DNA consisting of 0.45–0.55 μg of the indicated luciferase plasmid and 0.05 μg of the pRL-thymidine kinase control

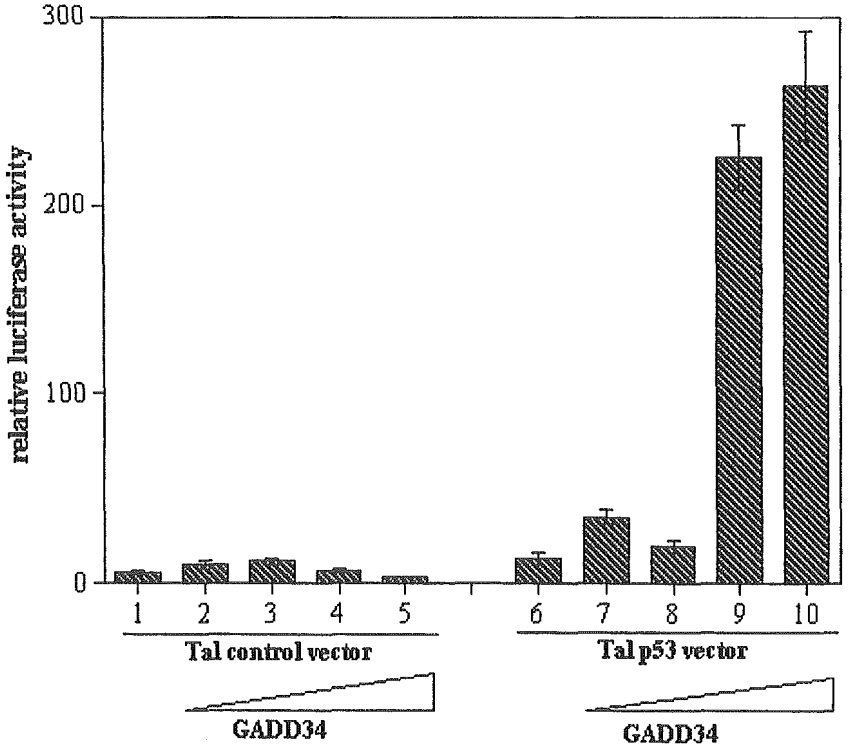

Fig. 2. Induction of Tal-p53 promoter activity by GADD34 transfection. Two hundred ninety-three cells were co-transfected with 0.05 μg of control vector (**lanes 1–5**) or 0.05 μg of Tal-p53 (**lanes 6–10**) and GADD34 expression vector (lanes 1–5 and lanes 6–10; 0, 0.05, 0.1, 0.25, 0.5 μg) in 24 tissue culture wells. Results were expressed as the mean ± standard errors (SE) of three independent experiments, each performed in triplicate.

vector (pRL-TK) (Promega, Southampton, England) per plate was used for transfection studies. After being harvested, the cells were assayed by the Dual-Luciferase Reporter Assay System (Promega), using a luminometer (Lumat; Berthold Technologies, Germany). Protein concentrations of the cell lysates were determined by the method of Bradford with the Bio-Rad protein assay dye reagent. Promoter activities were expressed as relative light units (RLU), normalized against the concentration of the protein. All transfection experiments were repeated three times.

Immunoprecipitation and Western Blotting

Human 293 cells in 6-well plates were transfected with 0.5μg each of the Myc-tagged pcDNA3.1/His-Myc (Invitrogen) expression plasmids. At 36 h after transfection, cells were dissolved in 1 ml of lysis buffer [25 mM Tris/HCl (pH 8.0) /150 mM NaCl/10% (v/v) glycerol/5 mM $MgCl_2$/2 mM EDTA/0.3% (v/v) Nonidet P40/ 5 mM NaF/0.5 mM PMSF/2 μg/ml aprotinin], and debris was discarded after centrifugation. Whole cell lysate was measured for protein quantity; 300 μg was used in the following steps: 1 μ (anti-MycSanta Cruz) of antibody was added to the lysates, which were then rotated at 4°C for 1 h. Then 20 μl of protein G/A—Sepharose beads was added and rotated for a further 2 h at 4°C. The beads were washed with lysis buffer three times and with PBS once. Proteins were eluted with SDS/PAGE sample buffer and boiled for 5 min. Western blotting was performed as described (Maehara et al., 2001) with the first antibodies, which were diluted 1:400 (anti-GADD34; Santa Cruz, CA) and 1:500 (anti-p21; Santa Cruz). Anti-p53 and anti-phospho Ser15-p53 (all rabbit polyclonal antibodies) were purchased from Cell Signaling Technology (New England Biolabs, Inc.).

RESULTS

GADD34 Induces p53 Phosphorylation

Previous studies have shown that the phosphorylation of p53 at Ser15 induces p53-dependent growth suppression [Fiscella et al., 1993].

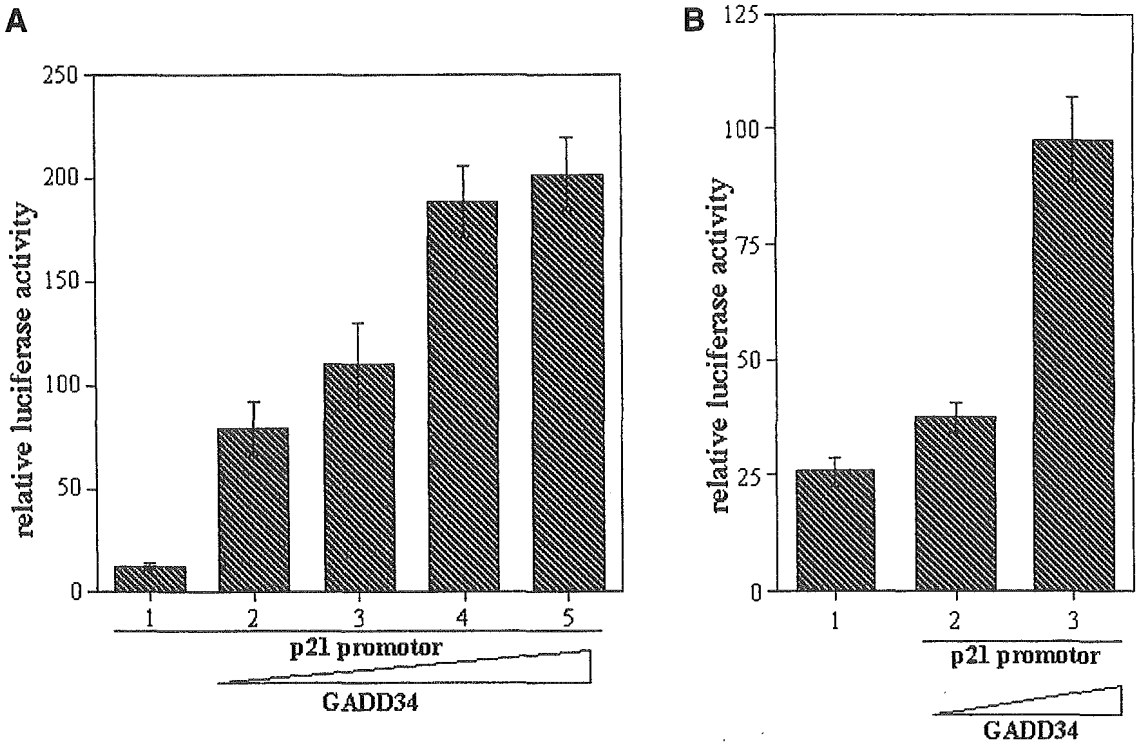

Fig. 3. Induction of p21/WAF1 promoter activity by GADD34 transfection. **A:** Two hundred ninety-three cells were co-transfected with 0.05 μg of p21/WAF1 promoter (**lanes 1–5**) and GADD34 expression vector (lanes 1–5; 0, 0.05, 0.1, 0.25, 0.5 μg) in 24-well tissue culture wells. Results were expressed as the mean ± SE of three independent experiments, each performed in triplicate. **B:** NIH3T3 cells were co-transfected with 0.05 μg of p21/WAF1 promoter (**lanes 1–3**) and GADD34 expression vector (lanes 1–3; 0, 0.05, 0.1 μg) in 24-well tissue culture wells. Results were expressed as the mean ± SE of three independent experiments, each performed in triplicate.

We first analyzed the phosphorylation of p53 induced by the transfection of GADD34 expression vector. We transfected Myc-tagged p53 together with increasing amounts of GADD34 into 293 cells. The phosphorylation of Ser15–p53 was increased by increasing the amount of GADD34 (Fig. 1A). Transfection of GADD34 also induced the endogenous phosphorylation of p53 (data not shown) and p53 protein expression (Fig. 1B).

Enhancement of Reporter Plasmid Containing p53 Responsive *Cis*-Element

Several target genes have p53-responsive *cis*-elements [El-Deiry et al., 1993; Thut et al., 1997; Zhao et al., 2001], such as GADD45, MDM2 and p21/WAF1. In order to examine whether GADD34 induces p53-responsive reporter plasmid, we transfected 293 cells with Tal–p53 reporter plasmid together with increasing amounts of GADD34 expression vector. The transfection of GADD34 up-regulates Tal–p53 promoter activity. (Fig. 2). Then we examined the expression of p21/WAF1, which is one of the target genes of p53 protein.

GADD34 Enhances the p21/WAF1 Promoter Activity

The expression of p21/WAF1 protein was increased by the GADD34 transfection (Fig. 1B). In order to determine whether or not p21/WAF1 promoter activity depends on GADD34, we cotransfected GADD34 expression vector with p21/WAF1 promoter. As shown in Figure 3, p21/WAF1 promoter activity was greatly enhanced by the increase of GADD34 transfection both in 293 cells (Fig. 3A) and NIH3T3 cells (Fig. 3B). Then in order to show that GADD34 induces p21/WAF1 promoter activity depends on p53, we used p53-deficient 10 (1) cells for promoter assay. Without p53 co-transfection, p21/WAF1 promoter activity was very low (Fig. 4, lane 5), and GADD34 co-transfection showed only a slight increase in promoter activity (Fig. 4,

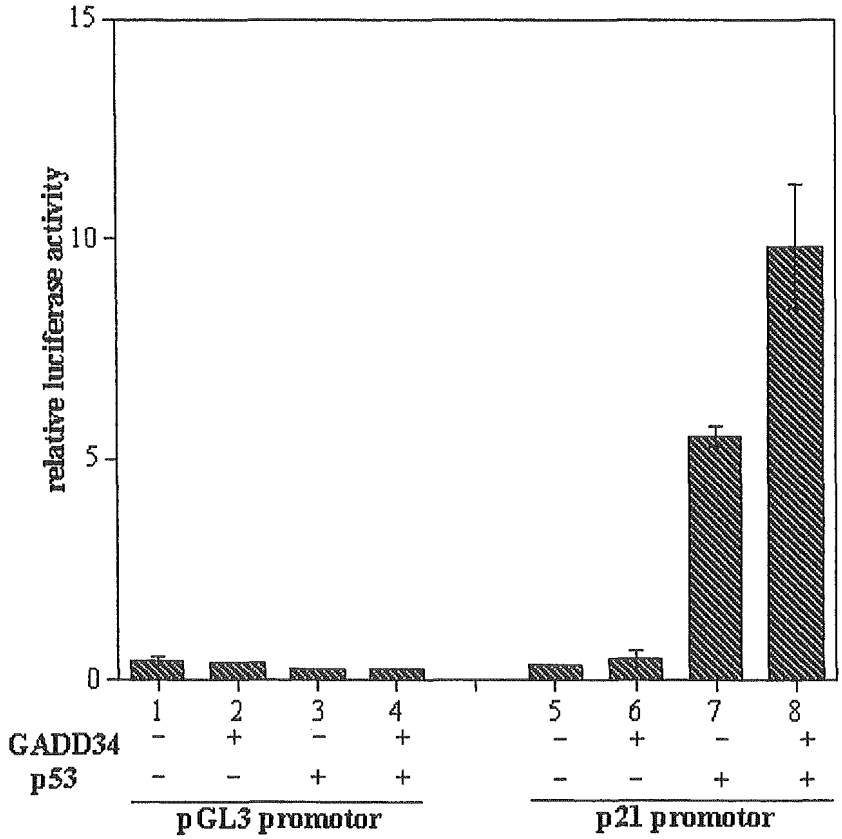

Fig. 4. GADD34-induced p21/WAF1 promoter activity in p53 deficient cells. Because p21 promoter vector was constructed in pGL3 luciferase vector, we used pGL3 vector as control. Promoter activities were measured in 10(1) cells transfected with 0.05 μg of control pGL3 promoter vector (**lanes 1–4**) or 0.05 μg of p21/WAF1 promoter vector (**lanes 5–8**) in 24 tissue culture wells. They were co-transfected with 0.25 μg of GADD34 expression vector (lanes 2, 6), 0.25 μg of p53 expression vector (lanes 3, 7), and 0.25 μg of each GADD34 and p53 expression vector (lanes 4, 8) Results were expressed as the mean ± SE of three independent experiments, each performed in triplicate.

lane 6). However, p53 transfection greatly enhanced p21/WAF1 promoter activity (Fig. 4, lane 7). Both p53 and GAD34 co-transfection produced a further enhancement of p21/WAF1 promoter activity (Fig. 4, lane 8). To further examine the p53 dependency of GADD34-induced p21/WAF1 promoter activity, we used the mutant of one of p53-binding sites (p21 (−1)). As shown in Figure 5, enhancement of p21 (−1)/WAF1 promoter activity by the p53 transfection (lanes 7,8) was lower than that of wild type p21/WAF1 promoter activity (lanes 11,12). Finally in order to show that GADD34 really induces p21/WAF1 transcription, we used GADD34-deficient mouse embryonic fibroblasts (MEF). Without GADD34 transfection, p21/WAF1 promoter activities were very low in GADD34 deficient MEF (Fig. 6, lane 3). The p21/WAF promoter activity was increased by the transfection of full length GADD34 cDNA (Fig. 6, lane 4).

DISCUSSION

Here, we showed that GADD34 induced p53 phosphorylation and p21/WAF1 reporter activities. Because GADD34 has been cloned as one of Growth arrest and DNA damage inducible proteins, it has been suggested that GADD34 induces cell cycle arrest or apoptosis. Hollander et al. [2001] showed that in a short-term transfection assay, more than 30% of GADD34-transfected cells exhibited nuclear fragmentation by 48 h. The most critical protein of cell cycle arrest is p21/WAF1. The transcription of p21/WAF1 is mainly regulated by p53 protein. Phospo-p53 binds to p21/WAF1 binding sites. Here, we showed that GADD34 induced p53 phosphorylation and p21/WAF1 reporter activities.

Others and we have shown that GADD34 interacts with a diverse array of proteins within the cell [Adler et al., 1999; Hasegawa et al., 1999; Hasegawa et al., 1999, 2000; Connor et al., 2001; Grishin et al., 2001]. Some of these interactions facilitate growth suppression/apoptosis. Expression of GADD34 in the colorectal cancer cell line SW480 has been reported to enhance IR-induced apoptosis [Adler et al., 1999]. In addition, the results of GADD34-induced apoptosis are extended to two other cell lines, HEK293 and HeLa, by the DNA-damaging agent MMS. These data suggest that GADD34 is a positive

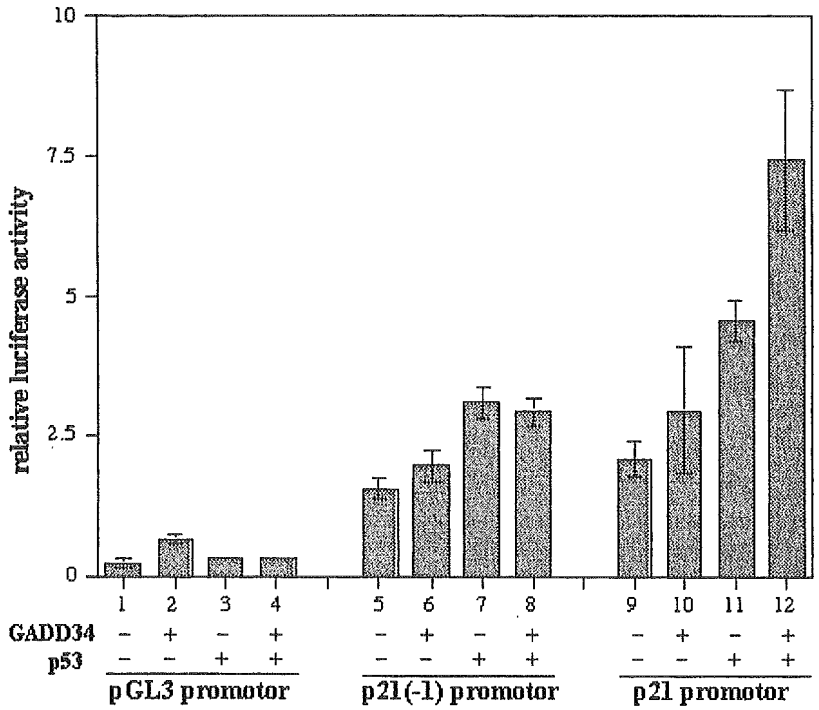

Fig. 5. Effects of p53-binding *cis*-elements in GADD34-induced p21/WAF1 promoter activity. 10(1) cells were transfected with 0.05 μg of pGL3 promoter vector (**lanes1–4**), 0.05 μg of p21(−1) promoter vector (**lanes 5–8**) or 0.05 μg of p21 promoter vector (**lanes 9–12**) in 24 tissue culture wells. They were co-transfected with 0.25 μg of GADD34 expression vector (lanes 2, 6, 10), 0.25 μg of p53 expression vector (lanes 3, 7, 11), and 0.25 μg of each GADD34 and p53 expression vector (lanes 4, 8, 12). Results were expressed as the mean ± SE of three independent experiments, each performed in triplicate.

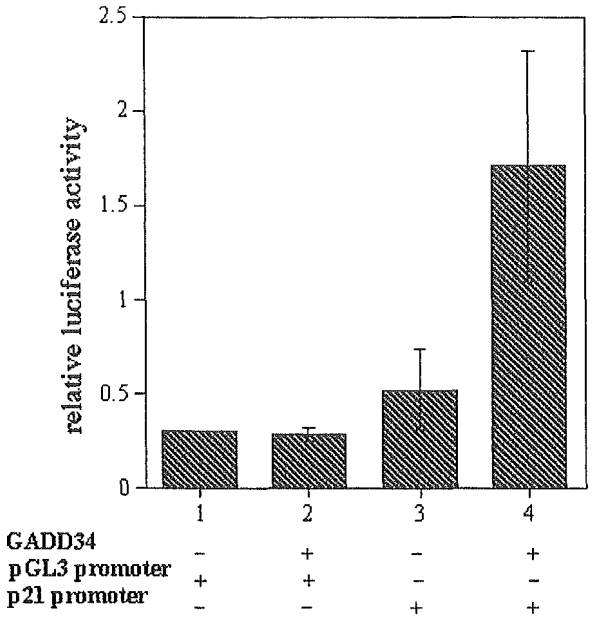

Fig. 6. Decreased p21/WAF1 promoter activity in GADD34-deficient MEF was recovered by GADD34 transfection. MEF were co-transfected with 0.05 μg of pGL3 promoter vector (**lanes 1, 2**) or 0.05 μg of p21/WAF1 promoter (**lanes 3, 4**), and control Myc-tagged vector (lanes 1, 3; 0.25 μg) or GADD34 expression vector (lanes 2, 4; 0.25 μg) in 24 tissue culture wells. Results were expressed as the mean ± SE of three independent experiments, each performed in triplicate.

regulator of apoptotic processes, whose activity is modulated by interaction with other proteins. It has been reported that human SNF5 protein (hSNF5/INI1) associates with GADD34, and that both proteins can coexist in a trimeric complex with chimeric leukemic HRX fusion proteins [Adler et al., 1999]. Lee et al. [2002] have shown that several subunits of the human SWI/SNF complex bind to the tumor suppressor protein p53 in vivo and in vitro. Overexpression of dominant negative forms of either hSNF5 or BRG-1 have inhibited p53-mediated cell growth suppression and apoptosis. These reports suggest that GADD34 itself induces apoptosis or cell cycle arrest. However, the molecular mechanisms or signaling cascades from GADD34 to apoptosis or cell cycle arrest have not been elucidated. Here we showed that GADD34 itself induced p53 phosphorylation and p21/WAF1 expression (Fig. 1). GADD34-induced p21/WAF1 expression was mainly dependent on p53 (Fig. 4). By using mutant of p21/WAF1 promoter, luciferase activity of p21/WAF1 was dependent on p53 binding site (data not shown). More precise biochemical mechanism of interaction between GADD34 and p53 are now ongoing.

Recently, it has been shown that human GADD34 has been induced by the differentiation and growth arrest of melanoma [Jiang et al., 2000] and glioma [Su et al., 2003]. Further adenovirus infection of melanoma differentiation-associated gene-7 (*mda-7*), which induces cell cycle arrest and apoptosis of melanoma, induces GADD34 via p38 MAPK phosphorylation [Su et al., 2003]. These works and our works presented here open the possibility to treat cancer by GADD34 induction.

REFERENCES

Adler HT, Chinery R, Wu DY, Kussick SJ, Payne JM, Fornace AJ, Jr., Tkachuk DC. 1999. Leukemic HRX fusion proteins inhibit GADD34-induced apoptosis and associate with the GADD34 and hSNF5/INI1 proteins. Mol Cell Biol 19:7050–7060.

Bai L, Merchant JL. 2001. ZBP-89 promotes growth arrest through stabilization of p53. Mol Cell Biol 21:4670–4683.

Brown SM, MacLean AR, McKie EA, Harland J. 1997. The herpes simplex virus virulence factor ICP34.5 and the cellular protein MyD116 complex with proliferating cell nuclear antigen through the 63-amino-acid domain conserved in ICP34.5, MyD116, and GADD34. J Virol 71:9442–9449.

Chin PL, Momand J, Pfeifer GP. 1997. In vivo evidence for binding of p53 to consensus binding sites in the *p21* and *GADD45* genes in response to ionizing radiation. Oncogene 15:87–99.

Connor JH, Weiser DC, Li S, Hallenbeck JH, Shenolikar S. 2001. Growth arrest and DNA damage-inducible protein GADD34 assembles a novel signaling complex containing protein phosphatase 1 and inhibitor 1. Mol Cell Biol 21: 6841–6850.

El-Deiry WS, Tokino T, Velculescu VE, Levy DB, Parsons R, Trent JM, Lin D, Mercer WE, Kinzler KW, Vogelstein B. 1993. WAF1, a potential mediator of p53 tumor suppression. Cell 75:817–825.

Fiscella M, Ullrich SJ, Zambrano N, Shields MT, Lin D, Lees-Miller SP, Anderson CW, Mercer WE, Appella E. 1993. Mutation of the serine 15 phosphorylation site of human p53 reduces the ability of p53 to inhibit cell cycle progression. Oncogene X:81519–1528.

Fornace AJ, Jr., Nebert DW, Hollander MC, Luethy JD, Papathanasiou M, Fargnoli J, Holbrook NJ. 1989. Mammalian genes coordinately regulated by growth arrest signals and DNA-damaging agents. Mol Cell Biol 9: 4196–4203.

Grishin AV, Azhipa O, Semenov I, Corey SJ. 2001. Interaction between growth arrest-DNA damage protein 34 and Src kinase Lyn negatively regulates genotoxic apoptosis. Proc Natl Acad Sci USA 28:10172–10177.

Harvey DM, Levine AJ. 1991. p53 alteration is a common event in the spontaneous immortalization of primary BALB/c murine embryo fibroblasts. Genes Dev 5:2375–2385.

Hasegawa T, Isobe K. 1999. Evidence for the interaction between Translin and GADD34in mammalian cells. Biochim Biophys Acta 1428:161–168.

Hasegawa T, Xiao H, Isobe K. 1999. Cloning of a GADD34-like gene that interacts with the zinc-finger transcription factor which binds to the p21(WAF) promoter. Biochem Biophys Res Commun 256:249–254.

Hasegawa T, Yagi A, Isobe K. 2000. Interaction between GADD34 and kinesin superfamily, KIF3A. Biochem Biophys Res Commun 267:593–596.

He B, Gross M, Roizman B. 1998. The g134.5 protein of herpes simplex virus 1 has the structural and functional attributes of a protein phosphatase 1 regulatory subunit and is present in a high molecular weight complex with the enzyme in infected cells. J Biol Chem 273:20737–20743.

Hollander MC, Zhan Q, Bae I, Fornace AJ, Jr. 1997. Mammalian GADD34, an apoptosis- and DNA damage-inducible gene. J Biol Chem 272:13731–13737.

Hollander MC, Sheikh MS, Yu K, Zhan Q, Iglesias M, Woodworth C, Fornace AJJ. 2001. Activation of Gadd34 by diverse apoptotic signals and suppression of its growth inhibitory effects by apoptotic inhibitors. Int J Cancer 96:22–31.

Jiang H, Kang DC, Alexandre D, Fisher PB. 2000. RaSH, a rapid subtraction hybridization approach for indentifying and cloning differentially expressed genes. Proc Natl Acad Sci USA 97:12684–12689.

Kojima E, Takeuchi A, Haneda M, Yagi A, Hasegawa T, Yamaki KI, Takeda K, Akira S, Shimokata K, Isobe KI. 2003. The function of GADD34 is a recovery from a shutoff of protein synthesis induced by ER stress-elucidation by GADD34-deficient mice. FASEB J. Jun 3 [Epub ahead of print].

Lee D, Kim JW, Seo T, Hwang SG, Choi EJ, Choe J. 2002. SWI/SNF complex interacts with tumor suppressor p53 and is necessary for the activation of p53-mediated transcription. J Biol Chem 277:22330–22337.

Maehara K, Oh-Hashi K, Isobe K. 2001. Early growth-responsive-1-dependent manganese superoxide dismutase gene transcription mediated by platelet-derived growth factor. FASEB J 10:1096/fj.00–0909fj.

Mengesdorf T, Althausen S, Oberndorfer I, Paschen W. 2001. Response of neurons to an irreversible inhibition of endoplasmic reticulum Ca(2+)–ATPase: Relationship between global protein synthesis and expression and translation of individual genes. Biochem J 356:805–812.

Novoa I, Zeng H, Harding HP, Ron D. 2001. Feedback inhibition of the unfolded protein response by GADD34-mediated dephosphorylation of eIF2alpha. J Cell Biol 153:1011–1022.

Novoa I, Zhang Y, Zeng H, Jungreis R, Harding HP, Ron D. 2003. Stress-induced gene expression requires programmed recovery from translational repression. EMBO J 22:1180–1187.

Su ZZ, Lebedeva IV, Sarkar D, Gopalkrishnan RV, Sauane M, Sigmon C, Yacoub A, Valerie K, Dent P, Fisher PB. 2003. Melanoma differentiation associated gene-7, mda-7/IL-24, selectively induces growth suppression, apoptosis and radiosensitization in malignant gliomas in a p53-independent manner. Oncogene 22:1164–1180.

Takeuchi A, Mishina Y, Miyaishi O, Kojima E, Hasegawa T, Isobe K. 2003. Heterozygosity with respect to Zfp 148 causes complete loss of fetal germ cells during mouse embryogenesis. Nat Genet 33:172–176.

Thut CJ, Goodrich JA, Tjian R. 1997. Repression of p53-mediated transcription by MDM2: A dual mechanism. Genes Dev 11:1974–1986.

Xiao H, Hasegawa T, Miyaishi O, Ohkusu K, Isobe K. 1997. Sodium butyrate induces NIH3T3 cells to senescence-like state and enhances promoter activity of p21WAF/CP1 in p53-independent manner. Biochem Biophys Res Commun 237:457–460.

Xiao H, Hasegawa T, Isobe K. 1999. Both Sp1 and Sp3 are responsible for p21WAF1 promoter activity induced by histone deacetylase inhibitor in NIH3T3 cells. J Cell Biochem 73:29–302.

Zhan Q, Lord KA, Alamo I, Jr., Hollander MC, Carrier F, Ron D, Kohn KW, Hoffmann B, Liebermann DA, Fornace AJ, Jr. 1994. The *gadd* and *MyD* genes define a novel set of mammalian genes encoding acidic proteins that synergistically suppress cell growth. Mol Cell Biol 14: 2361–2371.

Zhao H, Spitz MR, Tomlinson GE, Zhang H, Minna JD, Wu X. 2001. Gamma-radiation-induced G2 delay, apoptosis, and p53 response as potential susceptibility markers for lung cancer. Cancer Res 61:7819–7824.

Transcriptional Regulation of ILT Family Receptors[1]

Hideo Nakajima,[2]* Azusa Asai,* Aki Okada,* Lin Ping,[3]* Fumiyasu Hamajima,* Tetsutaro Sata,† and Kenichi Isobe*

Ig-like transcripts (ILT/leukocyte Ig-like receptor/monocyte/macrophage Ig-like receptor or CD85) are encoded on human chromosome 19q13.4, designated the human leukocyte receptor complex, and are predominantly expressed on myeloid lineage cells. We investigated the transcriptional regulation of ILT1, ILT2, and ILT4 genes to elucidate control mechanisms operating on the specific expression of ILT receptors. Inhibitory ILT2 and ILT4 both have a similar genomic structure, in which the ~160-bp 5′-flanking regions function as core promoters with critically important PU.1 binding sites. However, an Sp1 family-binding GC-box is more influential in *trans*-activation of ILT2 than ILT4. Additionally, ILT4 transcription is tightly regulated by chromatin modifications accompanied by histone acetylation, which strictly controls expression within myeloid lineage cells. Activating ILT1 carries a core promoter corresponding to the intronic region of ILT2 and ILT4, where PU.1 and Runx1 binding sites are essential, but a downstream heat shock element also augments promoter activity. Thus, each ILT is regulated by a distinct transcriptional mechanism, although PU.1 acts as a common *trans*-acting factor. We also found that human CMV infection strongly *trans*-activates inhibitory ILT2 and ILT4 genes through the expression of immediate-early proteins. *The Journal of Immunology,* 2003, 171: 6611–6620.

There is increasing evidence that hemopoietic cell function is modulated by the expression of several receptor families, which have both inhibitory and activating isoforms (1–4). These include Ig-like transcripts (ILT),[4] killer cell Ig-like receptor (KIR), and NKG2/CD94 receptor families. One subset of ILTs (ILT2, ILT3, ILT4, ILT5, and leukocyte Ig-like receptor 8) displays long cytoplasmic tails containing immunoreceptor tyrosine-based inhibitory motifs that inhibit cell activation by recruiting SH2-containing tyrosine phosphatase-1 (1). Another subset (ILT1, ILT7, ILT8, and leukocyte Ig-like receptor 6) contains short cytoplasmic domains lacking signal transduction motifs. Instead, they have a basic arginine residue within the transmembrane domain and associate with the FcR γ-chain, which transduces stimulatory signals (5). Inhibitory ILT2 and ILT4 have been shown to bind a broad range of HLA class I and nonclassical HLA-E and -G molecules. In addition, ILT2 binds to the viral class I-like molecule UL-18 encoded by human CMV (HCMV) (6). Genetically, functionally, and structurally, the ILT family is closely related to the KIR family, also mapped to leukocyte receptor complex (7–10). An outstanding property of ILTs is their cellular distribution, which greatly differs from that of KIRs expressed on NK cells and some T cells. All ILTs were shown to be expressed on myeloid lineage cells such as monocytes, macrophages, and dendritic cells (1). In addition, ILT1 and ILT5 are expressed on granulocytes and NK and T cell subsets, and ILT2 is broadly expressed on NK cells, T cells, and all B cells. In contrast, ILT4 expression is limited to myeloid cells. The expression of inhibitory ILT receptors increases during maturation of myeloid lineage cells, whereas the expression of activating ILT receptors remains stable or decreases slightly.

In this study we analyzed the 5′-flanking regions of well-characterized ILT genes, inhibitory ILT2, ILT4, and activating ILT1, and examined their promoter activities. Our investigation revealed that ILT2 and ILT4 shared homology of the core promoter and used similar *cis*-elements and *trans*-factors, whereas the Sp1 family-binding GC-box and histone acetylation at the core promoter locus largely affected the promoter activity of ILT2 and ILT4, respectively. Interestingly, the core promoter of ILT1 was located in the place corresponding to the first intronic regions of ILT2/4 and possessed a heat shock element. All promoters tested were predominantly activated in myeloid cells, and the transcription factor PU.1 played a critical role in *trans*-activation of all promoters. Thus, the expression of each ILT gene is controlled by distinct transcriptional regulation, with some similarities.

We also investigated other factors that can modulate transcription of ILTs. Our study showed that not only interactions between *cis*-elements and *trans*-factors, but epigenetic changes that alter chromatin structure also influence ILT gene expression, as often seen in many eukaryotic gene activation systems. Especially ILT4 expression is tightly regulated by histone acetylation at the core promoter locus that contributes to strictly controlled expression exclusively in myeloid lineage cells. In addition, interesting clinical observations were reported recently, suggesting that increased ILT2 expression on PBL preceded the development of HCMV disease after lung transplantation (11). In this study we demonstrate that HCMV immediate-early (IE) gene products vigorously *trans*-activate ILT2/4 promoters, providing new evidence that

*Department of Basic Gerontology, National Institute for Longevity Sciences, Obu, Aichi, Japan; and †Department of Pathology, National Institute of Infectious Disease, Shinjuku-ku, Tokyo, Japan

Received for publication May 21, 2003. Accepted for publication October 15, 2003.

The costs of publication of this article were defrayed in part by the payment of page charges. This article must therefore be hereby marked *advertisement* in accordance with 18 U.S.C. Section 1734 solely to indicate this fact.

[1] This work was supported by the Fund for Comprehensive Research on Aging and Health, a Research Grant for Longevity Sciences (13C-1) from the Ministry of Health and Welfare, the Program for Promotion of Fundamental Studies in Health Sciences of the Organization for Pharmaceutical Safety and Research, a grant from Japan Health Science Foundation, and grant-in-aids for Scientific Research from the Ministry of Education, Japan.

[2] Address correspondence and reprint requests to Dr. Hideo Nakajima, Department of Basic Gerontology, National Institute for Longevity Sciences, 36-3 Gengo, Morioka-Cho, Obu, Aichi 474-8522, Japan. E-mail address: hideonak@nils.go.jp

[3] Current address: Institute of Cancer Research, West China Hospital, Sichuan University Chengdu 6100041, China.

[4] Abbreviations used in this paper: ILT, Ig-like transcript; AcH3, acetylated histones H3; AcH4, acetylated histones H4; AZA, 5-aza-2′-deoxycytidine; ChIP, chromatin immunoprecipitation; DN, dominant negative; HCMV, human CMV; HDAC, histone deacetylase; HSF, heat shock transcription factor; IE, immediate early; KIR, killer cell Ig-like receptor; MZF-1, myeloid zinc finger gene-1; TSA, trichostatin A.

0022-1767/03/$02.00

HCMV can modulate the immune responses through up-regulation of inhibitory ILT genes.

Materials and Methods

Cells

Human embryonic kidney cell line 293 and mouse fibroblast cell line NIH-3T3 were maintained in DMEM with 10% FCS. Human myeloid cell lines (THP-1, U937, and K562), B cell lines (C1R and 721.221), and a T cell line (Jurkat) were grown in RPMI 1640 with 10% FCS.

Plasmid constructs

The ILT promoter constructions were generated by PCR using human genomic DNA as a template (Promega, Madison, WI). According to published genomic sequences, ~1-kb 5′-flanking regions of ILT1 (−1013 to +74), ILT2 (−994 to +27), and ILT4 (−1007 to +14) were amplified and ligated into the pGL3-basic vector (Promega) to generate ILT promoter-firefly luciferase reporter constructs. Various lengths of DNA fragments were further amplified and inserted. Reporter plasmids were mutated at the transcription factor-binding positions using PCR-based site-specific mutagenesis as follows (mutated residues are shown in lowercase letters): ILT2-Mu1, CCCaGaGGGTGGGGT; ILT4-Mu1, CCCGGGttGGAGGGA; ILT2/4-Mu2, AAAGaGaAA; ILT2/4-Mu3, AGAGaGa; ILT2/4-Mu4, CA CAAagCA; ILT1-Mu5, GTTGCAgagCCT; ILT1-Mu6, GTGTGaaT; and ILT1-Mu7, AGAgaGATC. PU.1 was amplified from a human leukocyte cDNA library, and PU.1ΔAD and PU.1-Ets were made by deletion of *trans*-activation domain Δ33–99 and all but the Ets domain Δ2–162, respectively, via PCR with appropriate primer pairs. All PU.1 constructs were ligated into pCDNA3.1 (Invitrogen, Carlsbad, CA). Transcription factor expression and backbone vectors were as follows: Sp1-pCGN (gift from Dr. T. Shenk, Princeton University, New Haven, CT), Runx1-pEF-BOS (provided by Dr. Y. Ito, Kyoto University, Kyoto, Japan), and myeloid zinc finger gene 1 (MZF-1)A,B-pCDNA3.1myc-his (received from Dr. J. Morris, Medical College of Wisconsin, Madison, WI). HCMV IE expression vectors pEQ274 (IE1), pEQ276 (IE1+2), pEQ326 (IE2), and control vector pEQ336 containing only the HCMV IE promoter without IE proteins were provided by Dr. A. Geballe (Fred Hutchinson Cancer Research Center, Seattle, WA).

Complementary DNA synthesis and RT-PCR amplification

Total RNA was isolated from 5×10^6 cells with RNeasy mini kits (Qiagen, Hilden, Germany) according to the manufacturer's instructions, and 10 μg of total RNA was subjected to cDNA synthesis using First-Strand cDNA synthesis kits (Amersham Pharmacia Biotech, Little Chalfont, U.K.). Mixtures containing 1 μl of serial 3-fold dilutions of synthesized cDNA were amplified by PCR for 20–30 cycles (94°C for 30 s, 60°C for 30 s, 72°C for 30 s) after denaturation for 3 min at 94°C. ILT1–4, PU.1, β-actin, GAPDH, and HCMV IE1 were amplified with specific sets of primers. Quantitative, real-time PCR was performed using the Smart Cycler System (Takara, Shiga, Japan). The relative amounts of cDNA in each sample were determined using a standard curve of known concentration. After normalization to GAPDH, the difference in quantity of a specific gene was calculated as the fold change from the control samples.

Luciferase assays

In general, 1×10^6 cells were plated in 500 μl of OPTI-MEM (Invitrogen) with 10% FCS in 24-well plates. Firefly luciferase reporter constructs (5 μg) and pRL-thymidine kinase control vector (pRL-TK; Promega; 0.25 μg) were mixed with 5 μl of Lipofectamine 2000 (Invitrogen) to form a complex. In cotransfection studies, mixtures also contained 1 μg of transcription factor expression plasmids, HCMV IE expression plasmids, or control vectors. Mixtures were added to cells, and after a 4-h incubation, 1 ml of fresh medium was added. Next day, the cells were harvested and assayed by the Dual-Luciferase Reporter Assay System (Promega), using a luminometer (EG&G, Berthold, Germany). The relative light units were calculated after normalization against *Renilla* luciferase activities of the pRL-TK internal control vector.

Primer extension

A 33-mer primer (ILT1,+62 to +29; ILT2/4, +69 to +36), which was complementary to the first exon of each ILT gene, was synthesized and end-labeled with [γ-^{32}P]ATP. Then 100 μg of total RNA and the primer were annealed for 2 h at 70–75°C in the Primer Extension Buffer (Promega). Next, the primer was extended for 1 h at 42°C with 1 U of AMV reverse transcriptase. The reaction products were loaded onto an 8% acrylamide gel under denaturing conditions, followed by autoradiography. A sequencing ladder of the ILT genome was made using the T7 Sequencing Kit (U.S. Biochemical Corp., Cleveland, OH) with the reporter plasmid as a template.

EMSAs

Nuclear extracts were prepared as previously described (12). Oligonucleotides corresponding to position 1 of ILT2 (−155 to −126), position 1 of ILT4 (−157 to −129), position 2 of ILT2 (−117 to −97)/ILT4 (−118 to −98), positions 5+6 of ILT1 (−74 to −49), position 6 of ILT1 (−63 to −49), and position 7 of ILT1 (−34 to −14) were generated and used as probes. Mutations were induced in the same manner as for the reporter constructs. Nuclear extract (5 μg) was incubated with 50 fmol of ^{32}P end-labeled probes at room temperature for 20 min. For competition assays, a 100-fold molecular excess of cold oligonucleotides was also added to the reaction mix. In supershift experiments, nuclear extracts were preincubated with 2 μl of Ab for 20 min at 4°C before adding the labeled probe. The polyclonal Abs and Sp1 consensus and mutant oligonucleotides were purchased from Santa Cruz Biotechnology (Santa Cruz, CA). Heat shock transcription factor (HSF) competitor oligonucleotides were previously described (13). DNA binding reactions were separated on 5% native polyacrylamide gels at 150 V for 60–240 min.

Chromatin immunoprecipitation assays (ChIP)

The ChIP procedure was performed according to the manufacturer's protocols (Upstate Biotechnology, Lake Placid, NY) with slight modifications. After the equivalent of 2×10^6 THP-1, U937, C1R, and 721.221 cells were cross-linked with 1% formaldehyde, cells were lysed in SDS lysis buffer and sonicated on ice. The length of the DNA fragments averaged 250–500 bp. Aliquots of equal volume from each sample were used as input controls. After intensive preclearing, immunoprecipitation was performed using specific Abs against acetylated histones H3 (AcH3) and H4 (AcH4) (Upstate Biotechnology) and PU.1 (Santa Cruz Biotechnology; 10 μl was used for each precipitation). After purification, DNA pellets were dissolved in 50 μl of H_2O, and 1 μl of serial 3-fold dilutions thereof was used for PCR amplification with 1 μCi [α-^{32}P]dCTP (30 cycles: 94°C for 30 s, 60°C for 30 s, 72°C for 45 s) after denaturation for 3 min at 94°C. The core promoter regions of ILT2 (−159 to −10) and ILT4 (−161 to −10) and upstream regions of the core promoter in ILT2 (−688 to −493) and ILT4 (−671 to −497) were amplified with specific sets of primers. PCR products were electrophoresed on 8% polyacrylamide gels.

Treatment of cells with 5-aza-2′-deoxycytidine (AZA), trichostatin A (TSA), and heat shock stimulation

Nuclear extracts were prepared from heat-shocked NIH-3T3 cells or THP-1 cells at 42°C for the indicated time and subjected to EMSA. For luciferase assays, 1 day after transfection of reporter plasmids, THP-1 cells were heat-shocked for 1 h at 42°C and allowed to recover at 37°C for 0, 2, and 4 h, respectively, before making lysates. For RT-PCR analysis, before total RNA extraction cells were treated with 0, 1, and 5 μM AZA (Sigma-Aldrich, St. Louis, MO) for 48 h or 100 ng/ml TSA (Sigma-Aldrich) for 15 h or were heat-shocked for 1 h at 42°C, followed by 2-h recovery at 37 °C.

HCMV infection

The AD169 strain of HCMV was used for infection. THP-1 and U937 were infected at multiplicities of infection of 20 PFU/cell for 6 h at 37°C and maintained in RPMI 1640 with 10% FCS. After 48-h incubation, total RNA was extracted and subjected to RT-PCR analysis.

Results

Genomic organization of ILT promoters

According to the database (GenBank accession no. AC009892, AC010518, NM006866, AF004230, and XM 008961) and some previous reports (7, 9), ILT2 and ILT4 have a 5′-untranslated exon like other ILTs, whereas translation of ILT1 is started in the first exon (Fig. 1*A*). To determine the precise transcription initiation sites, primer extension was performed (Fig. 1*B*). Alignments of nucleotides with genomic sequences indicated that the major transcription initiation site was a C residue at ~75 nt upstream of the ATG initiation codon in ILT1 and a G residue at ~600 nt upstream of the ATG in ILT2 and ILT4 (Fig. 1*B*, large arrow), whereas several minor transcription initiation sites were observed (small arrow). We set the major transcription initiation sites as +1.

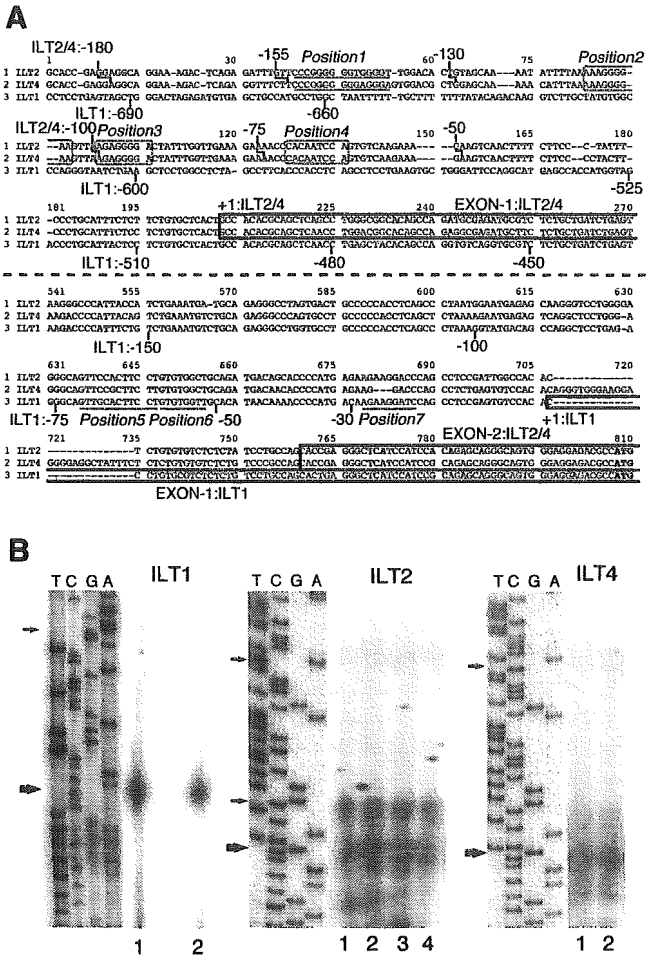

FIGURE 1. Comparison of ILT promoter gene structures. *A*, Alignment of nucleotides of the genomic sequence between the ATG initiation codon and ~800 bp upstream is shown. Exon structures are boxed with bold lines, transcription initiation sites are set as +1, and putative transcription factor binding sites are indicated in italics. *B*, Primer extension analysis of ILTs. Total RNA from THP-1 (*lanes 1*), U937 (*lanes 2*), C1R (*lane 3*), and 721.221 (*lane 4*) were used for extension. The major and minor extension products are shown by large and small arrows, respectively. The DNA sequence of each ILT is on the *left*.

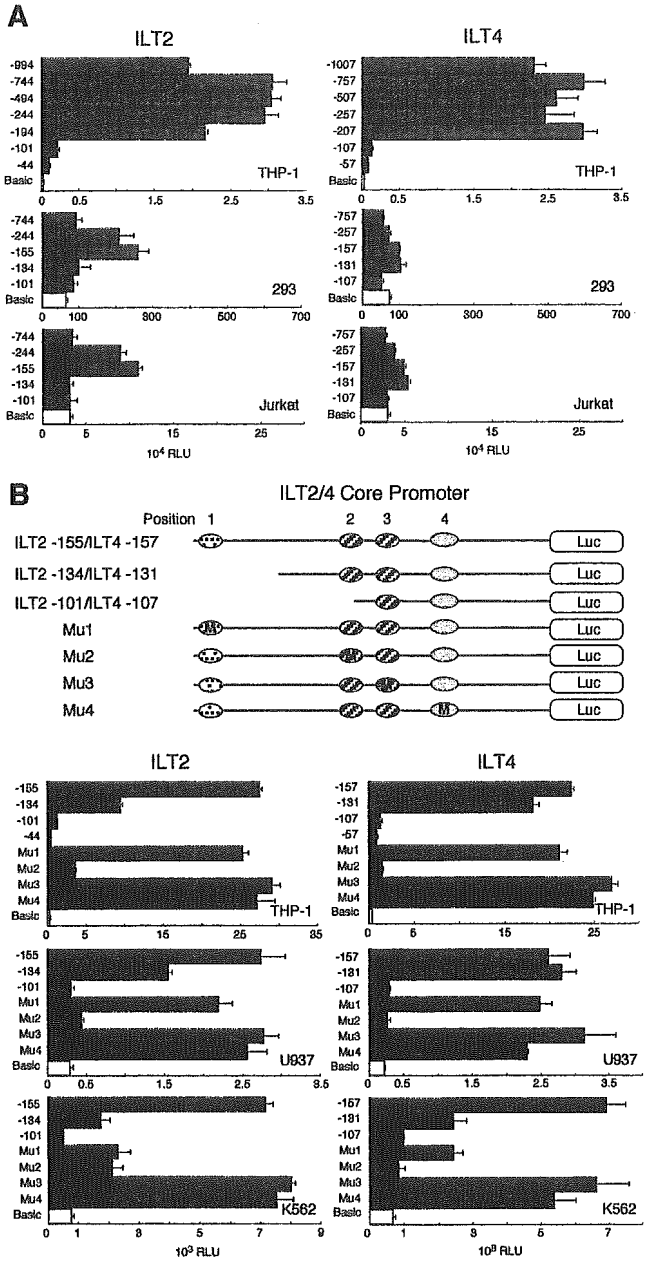

FIGURE 2. Promoter analysis of ILT2 and ILT4. *A*, Reporter assays on 5′-upstream regions of ILT2 and ILT4. THP-1, Jurkat, and 293 cells were transfected with a series of luciferase reporter constructs containing the 5′-flanking DNA of ILT2 and ILT4 genes. The relative light units (RLU) are shown after normalization against activity of the pRL-TK internal control vector. The RLU of promoterless pGL3-Basic are shown (□). The mean ± SD from quadruplicates are indicated. *B*, Analysis of minimal regions of ILT2 and ILT4 promoters. THP-1, U937, and K562 cells were transfected with reporter constructs of 5′-deletion or substituted mutants as illustrated, and luciferase activities were measured (RLU ± SD).

Cis-*elements in ILT2 and ILT4 promoters*

To identify regulatory elements, we performed luciferase assays with sets of ILT2 and ILT4 promoter-containing constructs. As shown in Fig. 2*A*, the ~1-kb 5′-flanking region of ILT2/4 demonstrated significant transcriptional activities in the myeloid cell line THP-1, exhibiting 50- to 150-fold activities compared with the promoterless Basic. In contrast, the epithelial cell line 293 and the T cell line Jurkat conferred very little or no transcriptional activity. A deletion up to position −160 resulted in no significant alteration; however, truncation up to −100 led to a drastic reduction of promoter activities in THP-1 (Fig. 2, *A* and *B*). These findings indicate that the proximal ~160 bp is the core promoter for ILT2/4.

According to our database search (http://www.cbrc.jp/research/db/TFSEARCHJ.html and http://tfbind.ims.u-tokyo.ac.jp), there are several transcription factor binding sites in the core promoter region of ILT2/4 (Fig. 1*A*). Position 1 is a GC-box known to interact with Sp1 family proteins, positions 2 and 3 have MZF-1-binding motifs, and position 4 has a GATA family-binding motif. To identify the *cis*-elements precisely, site-directed mutants of each position as well as 5′-deletion mutants were generated and tested in three myeloid cell lines (Fig. 2*B*). Although the effects of mutations varied in the cell lines tested, mutation or complete deletion of position 2 consistently led to a large reduction in transcriptional activities of both ILT2 and ILT4 down to almost the basal level. ILT2 position 1 was as influential as position 2 in K562, whereas it was less effective in THP-1 and U937. Position 1 of ILT4 had no effect or only minor effects on transcriptional activities in THP-1 and U937. In K562, abrogation of position 1 caused a >50% decrease in ILT4 transcriptional activity, although it was less effective than position 2. Mutation of either position 3

or 4 had no consistent or significant effect on promoter activities. Taken together, these data suggest that position 2 is the essential *cis*-element for the basal transcription of ILT2/4 genes, whereas position 1 has less effect, especially in ILT2.

Nuclear factors involved in ILT2/4 trans*-activation*

ILT2/4 position 2, the most important *cis*-element, is thought to interact with MZF-1, which is present as two splice variants, MZF-1A and MZF-1B (14). However, even using overexpressed nuclear extracts, we failed to detect binding of MZF-1 to position 2 (data not shown). Because position 2 also has an *ets* family transcription factor-binding motif, GGA(A/T) (Fig. 1*A*), we performed supershift EMSA with anti-Ets family Abs (Fig. 3*A*). In THP-1 and U937, nuclear proteins formed large complexes with the position 2 probe, but not with a mutant probe (Mu2). Most complexes were supershifted by anti-PU.1 (*lane 4*). Nuclear extracts from Jurkat formed few bands, which were weakly supershifted by anti-Ets1/2 (*lane 2*). Next, to examine the proteins binding to ILT2/4 position 1, EMSA was performed using THP-1 nuclear extracts (Fig. 3*B*). ILT2 position 1 nucleotides formed several bands, and high m.w. bands were supershifted by anti-Sp1 and -Sp3 (*left columns*, *lanes 2* and *3*), and most bands were totally eliminated by adding anti-Sp1 and -Sp3 together (*lane 4*) or in the presence of an excess amount of Sp1 consensus oligos (*lane 5*). ILT4 position 1 nucleotides showed similar binding specificities, although they were less clear (*right columns*, *lanes 1–6*). Considering that the sequence of position 1 was slightly different in ILT2 and ILT4 (Fig. 1*A*), and position 1 of ILT2 was more influential than the same position in ILT4 (Fig. 2*B*), some differences in binding properties must exist. For this reason we further tested competition and supershift EMSA using the ILT2 position 1 probe with a 100-fold excess of cold ILT4 position 1 nucleotides and vice versa (Fig. 3*B*, *lanes 7-12*). Despite competition with excessive ILT4 position 1 nucleotides, significant amounts of Sp1 family proteins were still bound to the ILT2 position 1 probe, as shown by supershifts with anti-Sp1, anti-Sp3, or both (*left columns*, *lanes 8–10*) and competition with Sp1 consensus oligos (*lane 11*). In contrast, ILT4 position 1 probe did not show any binding of Sp1 family proteins in competition with ILT2 position 1 nucleotides (*right columns*, *lanes 7–12*). These findings suggest that the affinity of ILT2 position 1 to Sp1 family proteins was much higher than that of ILT4 position 1.

Next, cotransfection studies were conducted. When PU.1 was introduced into PU.1-negative Jurkat cells, a large *trans*-activation of ILT2/4 promoters was observed (except for mutants at position 2 (Mu2); Fig. 3, *C* and *D*). MZF-1 and Sp1 essentially failed to *trans*-activate the ILT4 promoter (Fig. 3*C*), whereas Sp1 cotransfection induced a slight increase in ILT2 promoter activity and had additive effects to PU.1 on *trans*-activation in Jurkat (Fig. 3*D*, *left panel*). Cotransfection of Sp1 was as effective as PU.1 in THP1 cells, which possess endogenous PU.1 (Fig. 3*D*, *right panel*). Together the data show that PU.1 functioned as a potent *trans*-activator of ILT2/4 genes, but Sp1 had a weak and selective role. To further confirm the importance of the former, PU.1 dominant-negative mutants (PU.1-DN) were transfected into THP-1 cells (Fig. 3*E*). PU.1-DN caused a large reduction of ILT2/4 promoter activity by competition with endogenous PU.1.

Promoter analysis of ILT1

Transcription of ILT1 is initiated at the corresponding first intronic region of ILT2/4, whereas the 5′-upstream region of ILT1 has a sequence highly homologous to exon 1 of ILT2/4 (Fig. 1*A*). It is noteworthy that the genomic sequence of ILT1 distal from −525 is completely different. As shown in Fig. 4*A*, a series of constructs with the 5′-flanking region of ILT1 truncated up to −73 demonstrated significant transcriptional activity in THP-1, but very little in 293 and Jurkat. Moreover, constructs containing −663 to −484 or −763 to −484 corresponding to ILT2/4 promoter regions had no promoter activity, corroborating the evidence that ILT1 does not have a 5′-untranslated exon. Thus, the ILT1 core promoter exists within the proximal ~73 bp located at the intronic region of ILT2/4. According to a database search, there are three putative transcription factor binding sites, which we designated positions 5, 6, and 7 (Fig. 1*A*). They were predicted to interact with the Ets, Runx, and HSF families of transcription factors, respectively. Luciferase assays were performed with 5′-deletion and site-directed mutants introduced into the ILT1 core promoter (Fig. 4*B*). In all cell lines tested, mutation or deletion of position 5 caused profound defects in promoter activity. Mutation of position 6, adjacent to position 5, also led to a large decrease. In contrast, mutation of position 7 led to a 50% reduction in THP-1 and K562, but no reduction in U937. These findings indicate that positions 5 and 6 are the essential *cis*-elements in the ILT1 promoter, whereas position 7 functions only in certain cells.

Transcription factors that activate the ILT1 promoter

EMSA was conducted to identify transcription factors acting in ILT1. Because positions 5 + 6 are in close proximity, oligonucleotides consisting of both positions were used as a probe (Fig. 5*A*, *lanes 1-4*). A large amount of nuclear proteins formed complexes with the position 5+6 probe and were supershifted by anti-PU.1 or anti-Runx1 (small arrow, *lanes 2* and *3*). Relatively low m.w. bands were all shifted and disappeared by adding anti-PU.1 (*lanes 1* and *2*), whereas Runx1-containing complexes were adsorbed in the high density bands and could not be detected before the supershift (*lanes 1* and *3*). To confirm the Runx1 binding to position 6, probes with a mutation at position 5 (Mu5+6) or containing only position 6 were generated to eliminate position 5 binding proteins and were then subjected to supershift assays. Relatively high m.w. bands were clearly erased and supershifted by anti-Runx1 (*lanes 5–8*). It must also be noted that by adding anti-PU.1 and anti-Runx1 together to the position 5+6 probe, most binding complexes were further supershifted to the highest position (large arrow, *lane 4*), suggesting that the majority of PU.1 and Runx1 formed complexes with one another.

Position 7 is a heat shock element with an NGAAN motif (Fig. 1*A*). EMSA revealed that a high m.w. complex was formed with the position 7 probe in a heat shock-dependent manner (Fig. 5*B*). In NIH-3T3 cells, complexes were totally supershifted with anti-HSF1 and partially supershifted with anti-HSF2 (*lanes 5*, *6*, *8*, and *9*). In contrast, in THP-1, the HSF2-containing complex already formed, albeit in small amounts, with nuclear extracts from non-heat-shocked samples (small arrow, *lane 13*). This may explain the results of luciferase assays indicating that mutation of position 7 halved the promoter activity without heat shock treatment of THP-1 (Fig. 4*B*). After heat shock, a large amount of heat-responding proteins, recognized by anti-HSF1 Ab and competed against by specific competitor oligonucleotides, overwhelmed and replaced the HSF2-containing complex (Fig. 5*B*, *lanes 14–17*).

To define the significance of these transcription factors, we performed cotransfection and heat shock experiments. Cotransfection of PU.1 or Runx1 separately with the ILT1 −73 reporter plasmid resulted in a small increase (~1.3-fold) over background activity, but double transfection of PU.1 and Runx1 together had a marked effect (Fig. 5*C*). In addition, expression of PU.1-DN induced a remarkable decrease in luciferase activity. Cotransfection did not modulate the activity of the mutant at position 5 (Mu5) or of Basic.

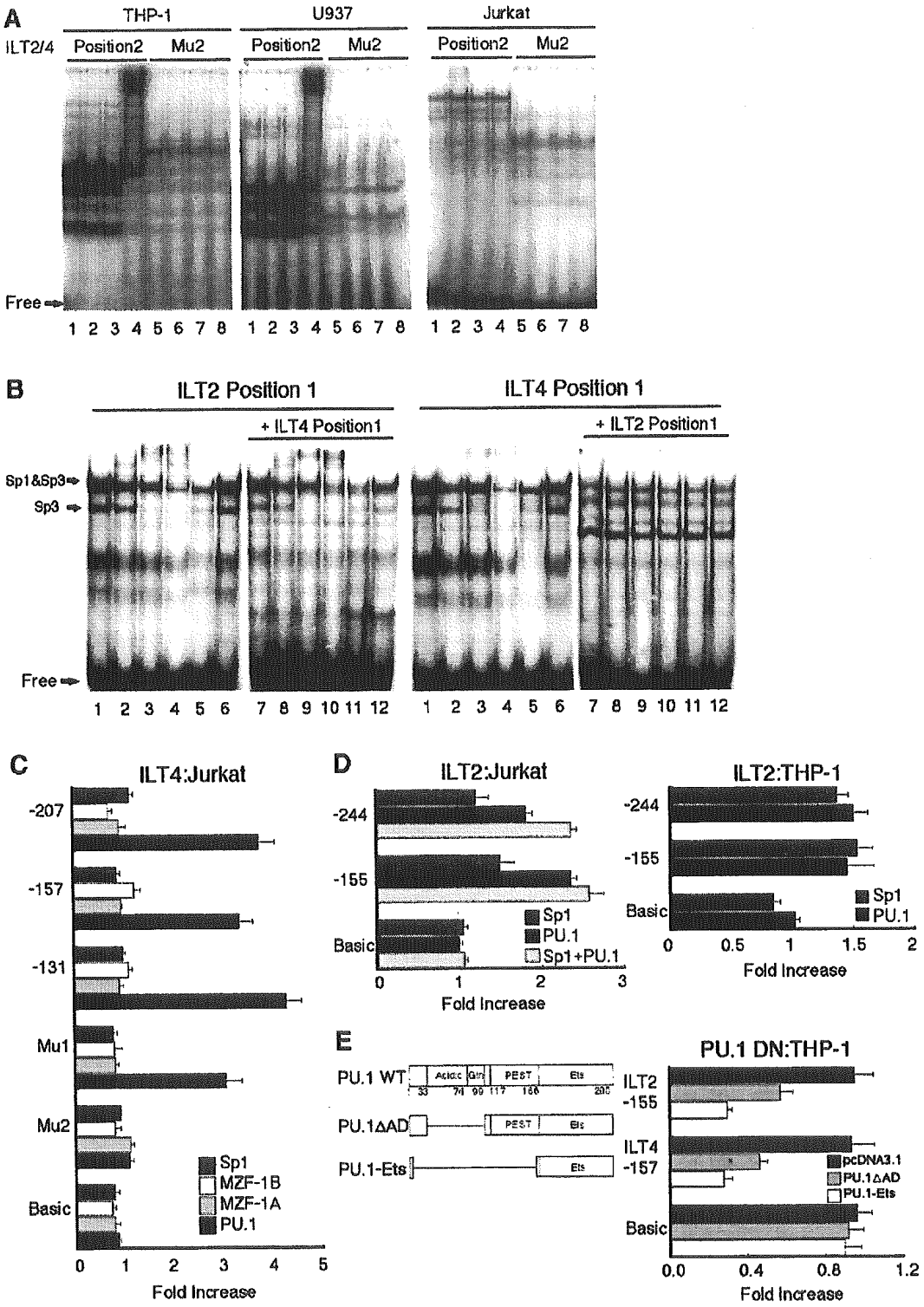

FIGURE 3. *A*, EMSA of ILT2/4 position 2. ILT2/4 position 2 and mutant (Mu2) probes were labeled and incubated with nuclear extracts from THP-1, U937, and Jurkat cells. Anti-Ets1/2 (*lanes 2* and *6*), anti-Elk (*lanes 3* and *7*), and anti-PU.1(*lanes 4* and *8*) were used for supershift assays. Reactions were separated on gels for 90 min (THP-1, U937) or 70 min (Jurkat). *B*, EMSA of ILT2 position 1 and ILT4 position 1. Nuclear extracts of THP-1 were used. Anti-Sp1 (*lanes 2* and *8*), anti-Sp3 (*lanes 3* and *9*), or both (*lanes 4* and *10*) were added for supershift, and Sp1 consensus (*lanes 5* and *11*) or mutant oligonucleotides (*lanes 6* and *12*) were added for competition. In addition, a 100-fold excess of cold ILT4 position 1 oligonucleotides was mixed with the labeled ILT2 position 1 probe for competition and vice versa (*lanes 7–12*). Gels were run for 70 min. *C*, *Trans*-acting candidates -PU.1, Sp1, MZF-1A, and MZF-1B were cotransfected into Jurkat with ILT4 reporter constructs. The relative light units (RLU) of transfectants with reporter plasmids and backbone vectors was set at 1, and fold increases in transcription factor transfectants are shown (mean ± SD). *D*, Reporter assays of ILT2 with transcription factors. Sp1, PU.1, or both were cotransfected into Jurkat (*left panel*) and THP-1 (*right panel*) with ILT2 constructs. The fold increase in RLU against backbone vector transfectants is shown. *E*, Effect of PU.1 dominant negative forms. PU.1ΔAD and PU.1-Ets were generated and used for cotransfection assay. RLU with only reporter plasmids was set at 1, and relative activities of cotransfectants are shown (mean ± SD).

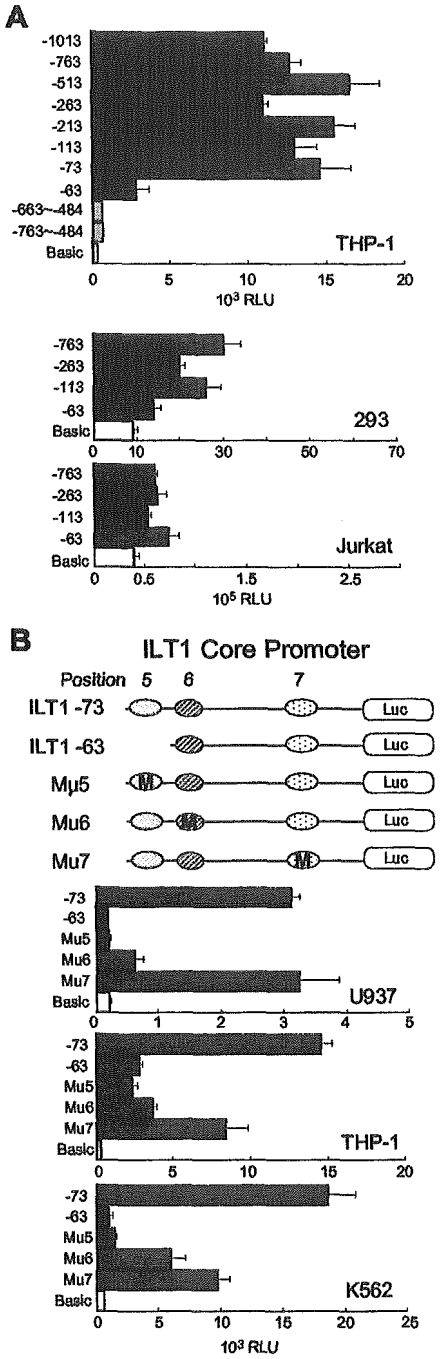

FIGURE 4. Promoter analysis of ILT1. *A*, Reporter assays on the 5′-upstream region of ILT1. In the same manner as described in Fig. 2*A*, THP-1, Jurkat, and 293 cells were transfected with a series of constructs containing the 5′-upstream region of ILT1. −663 to −484 and −763 to −484, corresponding to promoter regions of ILT2/4, are shown as light gray bars. Results are expressed as relative light units (RLU) ± SD of quadruplicate determinations. *B*, Core promoter analysis of ILT1. THP-1, U937, and K562 cells were transfected with 5′-deletion or substituted mutants of the ILT1 minimal promoter as illustrated, and luciferase activities were measured (RLU ± SD).

Together with EMSA analysis, these results suggested that PU.1 and Runx1 functioned cooperatively to *trans*-activate the ILT1 promoter. Immediately after heat shock, luciferase activities were reduced to one-third because protein synthesis was shut off (Fig. 5*D*, *upper panel*). However, luciferase activity of ILT1 −73 rose and reached a maximum after 2 h recovery at 37°C, showing a 1.5-fold increase compared with the untreated control. This rapid increase was not observed in the position 7 mutant (Mu7). We also investigated the effect of heat shock by quantitative, real-time PCR (Fig. 5*D*, *lower panel*). After 1-h heat shock treatment and 2-h recovery, only ILT1 increased significantly by ~3-fold in the message level.

Chromatin modification involved in ILT transcription

Because *cis*- and *trans*-interaction in the core promoter is not the sole element controlling gene expression, the B cell lines C1R and 721.221 did not express ILT4 despite possessing endogenous PU.1 (Fig. 6*A*, *upper panel*). Even after overexpression of PU.1 by transfection, ILT4 was still negative in C1R and Jurkat (*lower panel*). The discrepancy between reporter gene assays and endogenous transcription of ILT4 suggested that transcriptional activation was controlled by a higher order chromatin structure. Eukaryotic gene activation is dependent on chromatin modifications that facilitate access of *trans*-factors to cognate DNA binding sites. The amino-terminal tails of core histones are subjected to a large number of covalent modifications, including phosphorylation, acetylation, methylation, and ubiquitination. Histone acetylation, the best-described of these modifications, is positively correlated with transcriptional activation. In genomic DNA, the most relevant modification is cytosine methylation at CpG dinucleotides. Methylation of the promoter region CpG islands is associated with transcriptional silencing of imprinted genes. To examine the involvement of chromatin remodeling in ILT gene expression, THP-1 and C1R cells were treated with AZA (which promotes demethylation of CpG sites) or TSA (which inhibits histone deacetylases) and then subjected to RT-PCR analysis. As shown in Fig. 6*B*, a slight increase in ILT3 expression was observed in THP-1 after AZA treatment, but significant effects of AZA on the expression of the other ILTs were not observed, and ILT4 was still negative in C1R. In contrast, the ILT4 mRNA was markedly elevated after TSA stimulation in THP-1, although the message level of ILT1 to -3 did not increase greatly in either cell line (Fig. 6*C*). Surprisingly, after TSA treatment C1R now did express ILT4, albeit at very low levels (Fig. 6*C*, *lower panel*). To confirm that histone acetylation controls chromatin accessibility and transcription of ILT4, chromatin immunoprecipitation experiments were performed (Fig. 6*D*). After immunoprecipitation with anti-PU.1, -AcH3, and -AcH4, purified DNA was amplified by PCR to detect the core promoter regions of ILT2 (−159 to −10) and ILT4 (−161 to −10) and also the upstream regions of the core promoter in ILT2 (−688 to −493) and ILT4 (−671 to −497). The ILT2 core promoter locus (−159 to −10) was amplified comparably from precipitates of all four cell lines. In contrast, the ILT4 core promoter locus (−161 to −10) was markedly amplified in precipitates from the myeloid cell lines THP-1 and U937, but very little or not at all in the B cell lines C1R and 721.221. These results demonstrated that high levels of histone acetylation and chromatin opening at the ILT2 core promoter locus were present in both myeloid and B cell lines, but at the ILT4 core promoter locus these were largely limited to myeloid cell lines. In contrast, when immediate upstream regions of the core promoter locus were amplified from anti-AcH4 precipitates, no major differences were observed between myeloid cell lines and B cell lines or between ILT2 (−688 to −493) and ILT4 (−671 to −497). Thus, the ILT4 core promoter locus was hypoacetylated in nonmyeloid cell lines, but the lower levels of acetylation were not present across the entire ILT4 locus. Taken together, these findings indicate that ILT4 transcription is strictly regulated by histone acetylation that facilitates chromatin accessibility of the core promoter locus.

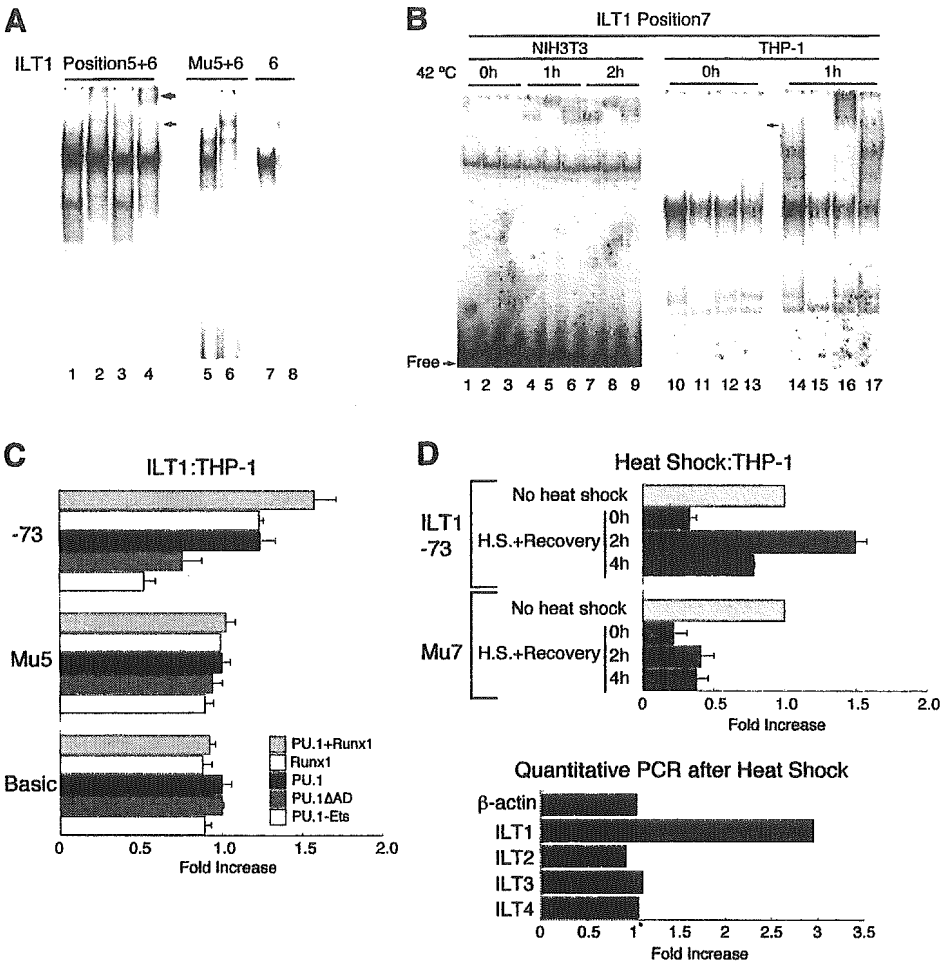

FIGURE 5. *A*, EMSA of ILT1 position 5 and position 6. THP-1 nuclear extracts were incubated with a probe of ILT1 positions 5+6 (*lanes 1–4*), Mu5+6 (substituted mutation at position 5; *lanes 5* and *6*), or position 6 (*lanes 7* and *8*). Supershift EMSA was performed using anti-PU.1 (*lanes 2* and *4*) and anti-Runx1 (*lanes 3*, *4*, *6*, and *8*). Gels were run for 90 min. *B*, EMSA of ILT1 position 7. NIH-3T3 and THP-1 cells were heat-shocked for the indicated period, and nuclear extracts were subjected to EMSA. Anti-HSF1 (*lanes 2*, *5*, *8*, *12*, and *16*) and anti-HSF2 (*lanes 3*, *6*, *9*, *13*, and *17*) were used for supershift, and oligonucleotide binding to HSF were used for competition (*lanes 11* and *15*). Samples were separated on gels for 70 min (NIH-3T3) and 240 min (THP-1), respectively. *C*, Expression vectors of PU.1, Runx1, and PU.1-DN were cotransfected into THP-1 cells with reporter plasmids. Relative activities of cotransfectants against backbone vector transfectants are shown (mean ± SD). *D*, One day after transfection with ILT1 reporter constructs, THP-1 cells either were heat-shocked for 1 h, followed by recovery at 37°C in the time course, or were not heat-shocked. The relative light units (RLU) of untreated samples was set at 1, and the relative activity of heat-shocked samples is shown (mean ± SD; *upper panel*). After 2-h recovery from heat shock, RNA was extracted from THP-1, and quantitative, real-time PCR was performed. The quantity of specific gene product was normalized to GAPDH, and the differences are expressed as fold increases over untreated samples (*lower panel*).

HCMV strongly trans*-activates ILT2 and ILT4 expression*

It was recently reported that increased expression of ILT2 was evident in patients who developed HCMV disease after lung transplantation. This elevation was observed several weeks before virus DNA could be detected in serum and might be an early identification of HCMV disease (11). In addition, it was demonstrated that murine Ig superfamily gp49B inhibitory receptors, homologues of KIR, were up-regulated on NK cells after murine CMV infection (15). HCMV IE proteins, IE1 and IE2, either independently or synergistically, are reported to activate the transcription of many cellular genes by direct binding to DNA or interaction with transcription factors such as Sp1, TBP, p300, c-Jun, and PU.1 (16–20). Therefore, the expression of ILTs could also be modulated by HCMV infection through IE-mediated *trans*-activation. As previously reported, THP-1 and U937 could not be productively infected, but successfully expressed IE genes 48 h after virus exposure (Fig. 6*E*). After infection, significantly higher levels of ILT2 and ILT4 expression were observed. At the same time, the effect of HCMV infection on ILT1, ILT3, or β-actin expression was far less, if any. To clarify the mechanism of HCMV-induced up-regulation of ILTs, we performed luciferase assays with cotransfection of HCMV IE expression vectors (Fig. 6*F*). IE1 alone slightly up-regulated all promoter activities, whereas IE2 alone did so less effectively. However, IE1 and IE2 synergistically *trans*-activated ILT2 and ILT4 promoters to a significant degree, but this was not observed in ILT1. These results were compatible with RT-PCR analysis, supporting the evidence that HCMV largely enhanced transcriptional activity of ILT2 and ILT4 genes through IE expression.

Discussion

In the present study we have demonstrated the importance of PU.1 in *trans*-activating all ILT promoters investigated. PU.1 (also termed Spi-1) is a hemopoietic-specific *ets* family transcription factor required for the development of both myeloid and lymphoid lineages (21–25). PU.1 expression is detectable even in multipotent hemopoietic stem cells and is up-regulated during myeloid and B cell differentiation. Considering that there are a number of genes

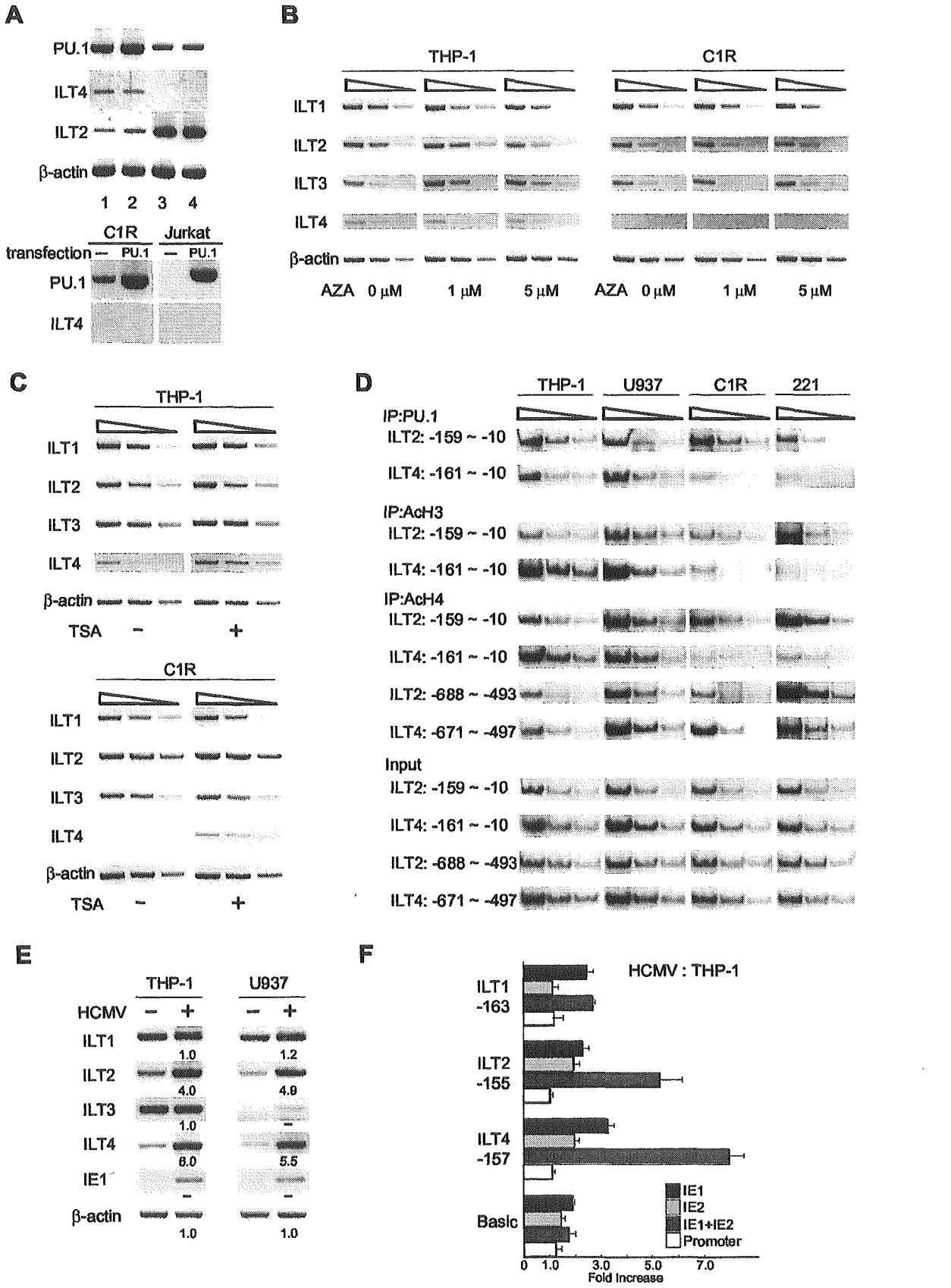

FIGURE 6. Other factors that modulate ILT transcription. *A*, RT-PCR analysis. ILT2, ILT4, and PU.1 were amplified from cDNA of THP-1 (*lane 1*), U937 (*lane 2*), C1R (*lane 3*), and 721.221 (*lane 4*). Amplified β-actin is shown as a control (*upper panel*). C1R and Jurkat transfected with PU.1 were also subjected to RT-PCR (*lower panel*). *B*, THP-1 and C1R cells were incubated in the presence of 0, 1, or 5 μM AZA for 48 h, and RT-PCR analysis was performed. ILT1 to -4 genes were amplified from synthesized cDNA that was serially diluted. *C*, THP-1 and C1R cells were either treated with TSA (100 ng/ml) for 15 h or left untreated, followed by RT-PCR analysis. *D*, ChIP assay. Abs to PU.1, AcH3, and AcH4 were used for chromatin immunoprecipitation from THP-1, U937, C1R, and 721.221. PCR was performed to amplify the core promoter regions of ILT2 (−159 to −10) and ILT4 (−161 to −10) and their upstream regions in ILT2 (−688 to −493) and ILT4 (−671 to −497) from serially diluted samples. Input corresponded (*Figure legend continues*)